Vehicle Impact Attenuation By Modular Crash Cushion

By
T. J. Hirsch
Research Engineer and Principal Investigator
and
Don L. Ivey
Associate Research Engineer

Research Report Number 146-1

Studies of Field Adaptation
of Impact Attenuation Systems

Research Study Number 2-8-68-146

Sponsored By
The Texas Highway Department
in cooperation with
The United States Department of Transportation, Federal Highway Administratio
Bureau of Public Roads

June, 1969

TEXAS TRANSPORTATION INSTITUTE
Texas A&M University
College Station, Texas

Abstract

The Modular Crash Cushion, in its first generation form, is an arrangement of 55-gallon tight head drums positioned to protect motorists from inadvertently driving into rigid obstacles. This protective device is a most crash worthy and economical vehicle impact attenuator. It has been subjected to five full-scale crash tests by the Highway Safety Research Center of the Texas Transportation Institute.

The occurrence of several single vehicle accidents at elevated exit ramps on the Interstate Highway System pointed out the need for such an impact attenuation system. This type of accident has occurred when motorists were traveling on the main freeway lanes and decided too late to try to turn right onto an off-ramp. The gore separating the off-ramp from the main lanes usually terminates in a reinforced concrete wall which anchors the bridge railing. This railing prevents motorists from inadvertently driving over the side of the freeway. Misjudgment on the part of the motorist when attempting this turn can result in a collision with the concrete retaining wall in the gore, even though these retaining walls have been heavily delineated as danger zones. The recurrence of accidents following the same general pattern demonstrated the need for a protective impact attenuation system at these points.

The purpose of the Modular Crash Cushion is to stop a moving vehicle over a distance sufficient to allow a relatively low deceleration rate (12 to 18 feet). The proposed designs of this protective system were subjected to five full-scale vehicle crash tests—two of these tests were head-on, two were at an impact angle of 30°, and one was at an impact angle of 20°. These tests showed that the Modular Crash Cushion was highly effective in stopping a vehicle with acceptable levels of deceleration.

As a result of these tests, Modular Crash Cushions have been installed at four locations in Houston, two locations in Dallas, and contracts are being let for additional installations in Texas and other states. Figure 1 shows one of the Houston locations before and after the installation of the Modular Crash Cushion.

Acknowledgments

This study was conducted under an interagency contract between the Texas Transportation Institute and the Texas Highway Department. It was sponsored jointly by the Texas Highway Department and the Bureau of Public Roads. Liaison was maintained through Mr. John Nixon and Mr. Paul Tutt, contact representatives for the Texas Highway Department.

The work was carried out by personnel of the Highway Safety Research Center of Texas Transportation Institute under the direction of the principal investigator, Dr. T. J. Hirsch of the Structural Research Division of the Texas Transportation Institute.

The opinions, findings, and conclusions expressed in this publication are those of the authors and not necessarily those of the Bureau of Public Roads.

Table of Contents

Introduction

The occurrence of several single vehicle accidents at elevated exit ramps on the Interstate Highway system pointed out the need for this research program. This type of accident has occurred when motorists were traveling on the main freeway lanes and decided too late to try to turn right onto an off-ramp. The gore separating the off-ramp from the main lanes usually terminates in a reinforced concrete wall which anchors the bridge railing. This railing prevents motorists from inadvertently driving over the side of the freeway. Misjudgment on the part of the motorist when attempting this turn can result in a collision with the retaining wall in the gore, even though these retaining walls have been heavily delineated as danger zones. The recurrence of accidents following the same general pattern demonstrated the need for a protective impact attenuation system at these points.

A single test[1]* conducted previously by the Texas Transportation Institute had shown that an impact attenuation system composed of 55-gallon tight-head drums was extremely effective. The additional tests conducted in this study were to determine the reaction of specific barrel arrangements to both head-on and angle vehicle crashes. These specific arrangements were proposed for installation at elevated exit ramps in the Houston freeway system.

The purpose of the Modular Crash Cushion is to stop a moving vehicle over a distance sufficient to allow a relatively low deceleration rate. The proposed Modular Crash Cushions were subjected to five full-scale vehicle crash tests—two of these tests were head-on, two were at an impact angle of 30°, and one was at an impact angle of 20°. These tests showed that the Modular Crash Cushion could be highly effective in stopping a vehicle with acceptable levels of deceleration. As a result of these tests, Modular Crash Cushions have been installed at four locations in Houston, two locations in Dallas, and contracts are being let for additional installations in Texas and other states. Figure 1 shows one of the Houston locations before and after the installation of the Modular Crash Cushion.

*Refers to corresponding number in Selected References.

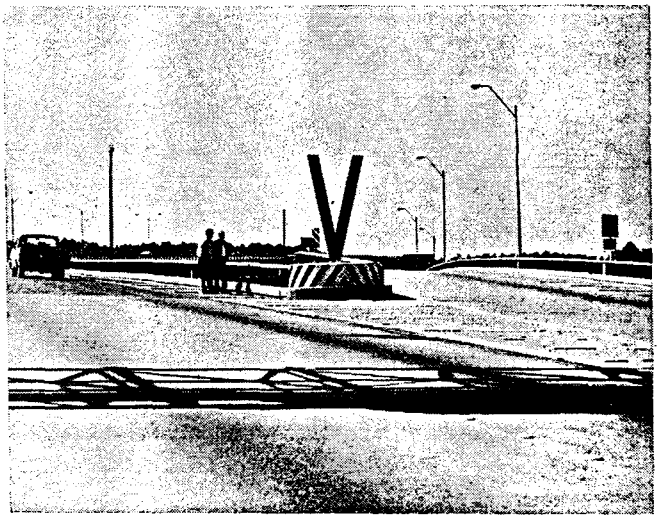

Before installation

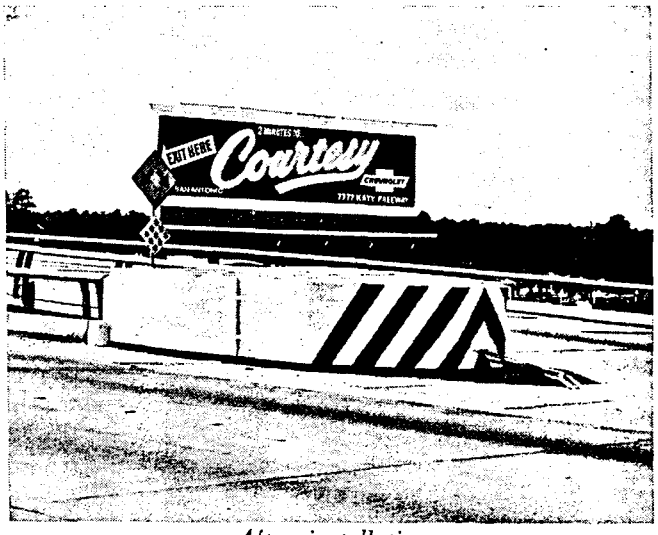

After installation

Figure 1. Installation site for modular crash cushion in Houston.

Details of Individual Tests

General

The Modular Crash Cushion which was used in Tests 1146-1, -3, and -4 is shown in Figure 2 protecting a rigid bridge pier. It is composed of 38 barrels which are welded together at top and bottom at every point where their rims meet. This weld connection is detailed in Figure 3. Also shown are details of how the top and bottom diaphragms of each barrel are cut out. These cut-outs are necessary to reduce the crushing strength of the barrel to the desired level (see Figure 4). The crash cushion is surrounded by three steel banding straps and is supported by reinforcing bar chairs. These re-bar chairs place the system at the desired elevation to prevent vehicle ramping (usually 4 to 6 in. above grade).

In order for the Modular Crash Cushion to take angular vehicle impacts, $\frac{5}{8}$ inch cables were tied to the simulated bridge pier and threaded between the rows of barrels. These cables were supported on the rolling hoops and tied off at a reinforced concrete anchor shaft located flush with the ground in front of the nose of the barrier. These cables are shown as dotted lines in Figure 2. The cables have the secondary function of holding the barrels close to the ground during a collision. The barrels must not be attached rigidly to the

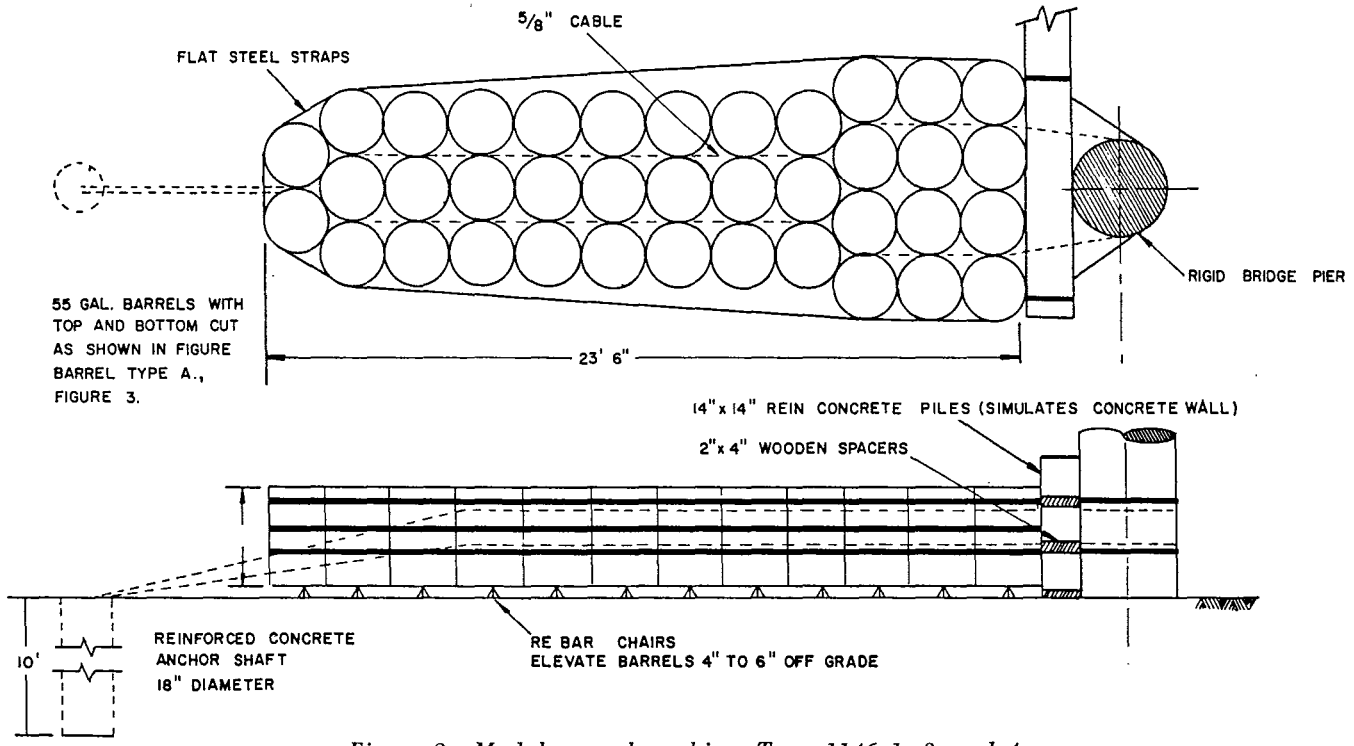

Figure 2. Modular crash cushion, Tests 1146 1, 3, and 4.

cable, but must remain free to slide down the cable during the vehicle impact.

Instrumentation of each test consisted of the following set ups. (1) Two high-speed cameras were located so that one camera gave a reliable determination of vehicle speed at impact, while the second gave the vehicle position at any time after impact. These high-speed cameras were operated at 500 frames per second. (2) Two documentary cameras were located at optimum observation points. Usually one of these cameras was

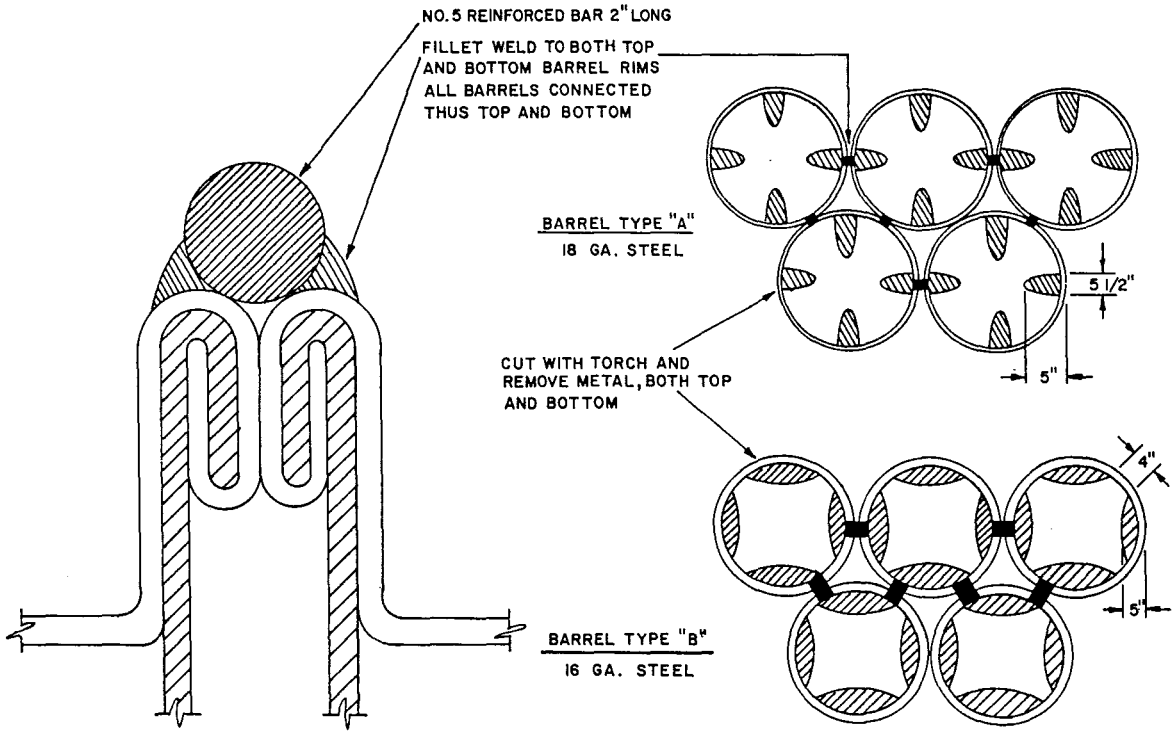

Figure 3. Detail of top and bottom of 55-gallon tight-head universal steel drum.

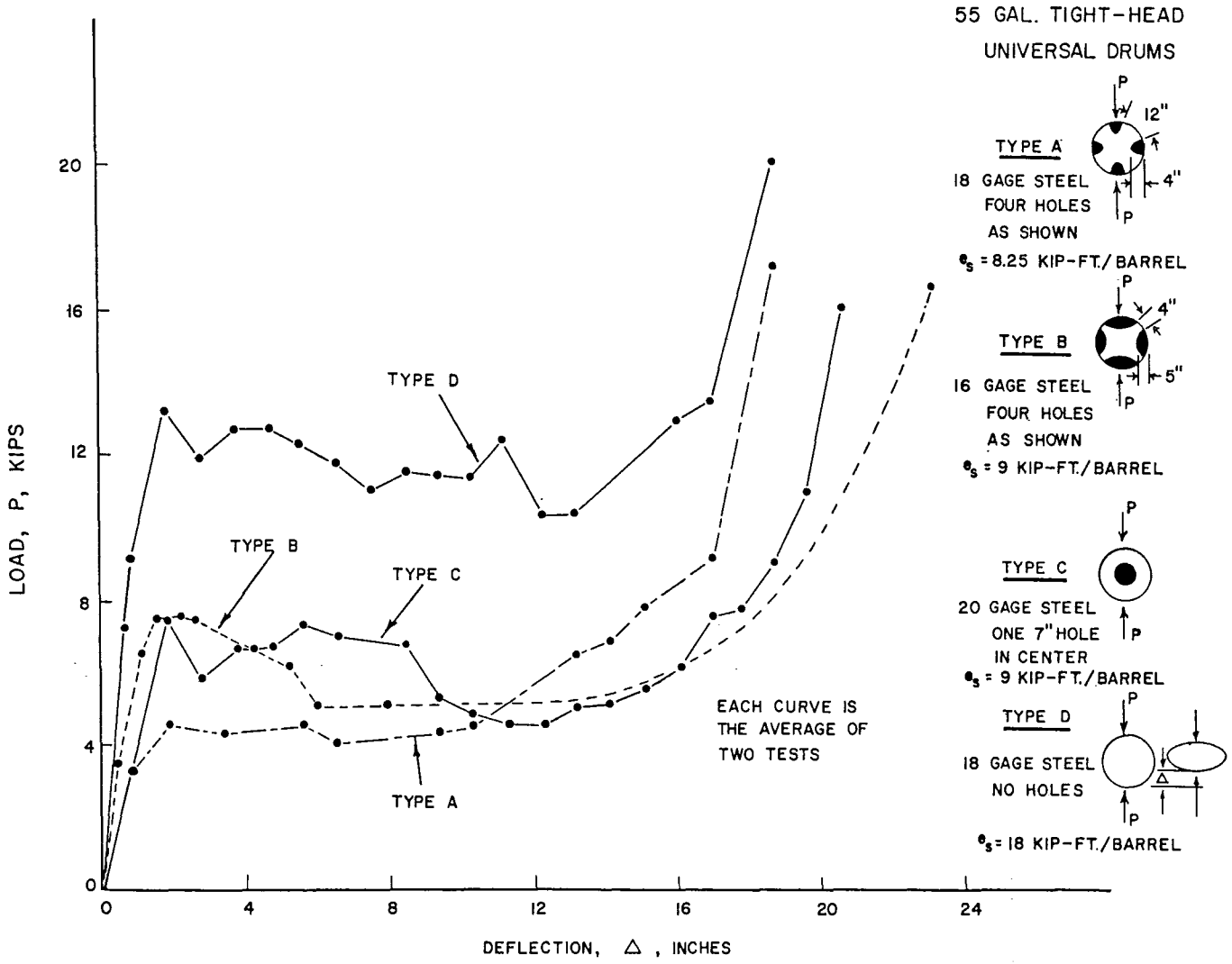

Figure 4. Load-deflection curves for 55-gallon drums.

located behind the barrier looking directly up the vehicle trajectory. The other was located at a height of 20 feet, on the side of the system which would be attacked. (3) Electronic accelerometers were attached to the frame of the vehicle and positioned in the chest cavity of the dummy. These accelerometers were oriented to give longitudinal and transverse accelerations. (4) An Impact-O-Graph was installed in the trunk of the vehicle which gave approximate accelerations in the longitudinal, transverse, and vertical directions. (5) A tape switch was located on the vehicle path slightly in advance of the contact point. This switch gave a reliable indication of vehicle speed which would be checked against the speed determined from the high-speed film. In addition to the determination of film speed using timing lights, timing clocks were included in the photographic field as a supporting time reference.

The detailed informational reporting of each test includes the following: (1) a summary sheet of the high-speed film data; (2) photographs of both the test vehicle and the Modular crash cushion before the test; (3) a drawing of the Modular Crash Cushion, as built; (4) sequential photographs of the test itself; (5) an overall view of the impact area after the test; (6) a position-time diagram showing graphically the vehicle position at various time intervals during the test and the initial and final barrier position; and (7) photographs of the damage to the vehicle and Modular Crash Cushion after the test. Additional information, such as tabular values of the high-speed film data and graphs of electronic acceleration data and accelerations by Impact-O-Graph, is given in the Appendix.

Test 1146-1

55-gallon drums with tops and bottoms cut, 3 rows four drums wide, 8 rows three drums wide and 1 row two drums wide, protecting rigid simulated bridge abutment (30° Test). See Figure 2.

Vehicle Weight = 3640 lbs (1958 Chevrolet, 4-Door).
Vehicle Velocity = 41.3 mph or 60.6 fps.
Change in Velocity = 41.3 mph or 60.6 fps.
Average Deceleration = 3.7 g's (longitudinal).
Duration of Impact:
To Deepest Penetration = 600 ms.
To Final Vehicle Position = 1220 ms.
Stopping Distance (Longitudinal) = 16.2 ft.
Angular Movement While Stopping = 106°.

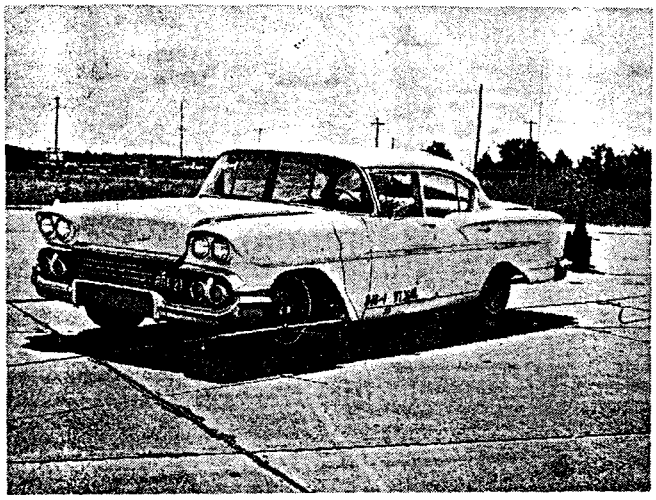

Figure 5. Vehicle before test (1146-1).

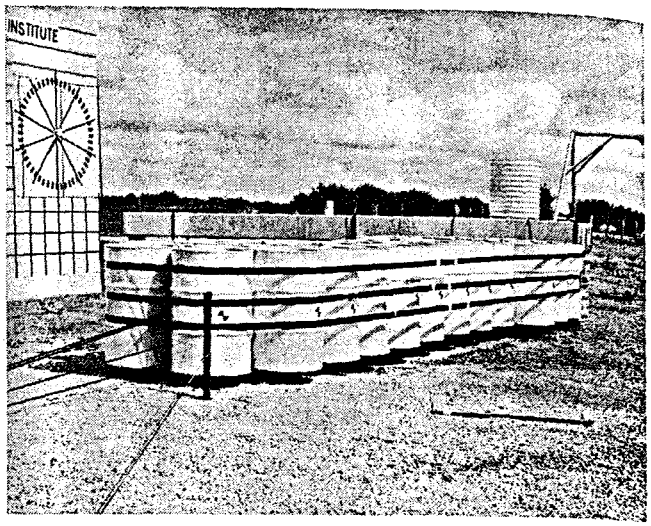

Figure 6. Modular crash cushion before test, installed in front of rigid barrier (1145-1).

The test vehicle was brought to a stop over a longitudinal distance of 16.2 ft at the very nominal deceleration level of 3.7 g's. This test cannot be considered representative, however, because of a structural failure which occurred during the collision. The cable anchorage which is in advance of the nose of the system was torn loose during the test and permitted the crash cushion to rotate away from the vehicle, thus reducing the resistance to the vehicle's penetration (see Figure 7, Photographs 4 and 5). The rear of the vehicle swung around during the collision and the right side of the vehicle contacted the barrier as shown in Photograph 6 of Figure 7. If the vehicle's speed had been higher, a significant secondary collision might have occurred between the vehicle and the barrier. This test should indicate the necessity for an adequate cable anchorage to provide the Modular Crash Cushion with adequate lateral stability. Damage to the vehicle was nominal, with the left front fender deformed approximately 9 inches and minor damage to the hood and grill.

1

2

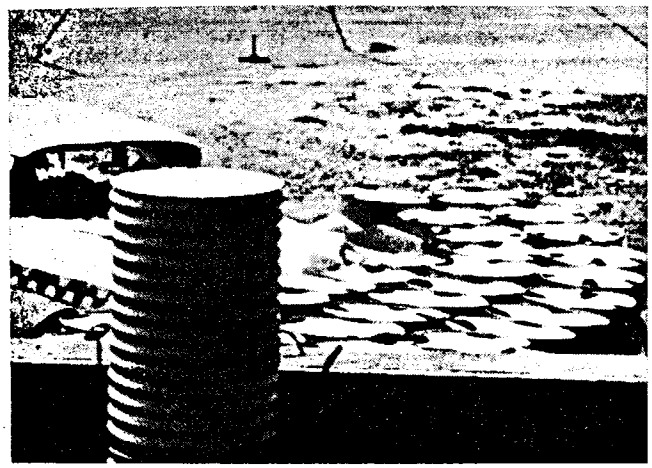

3

4

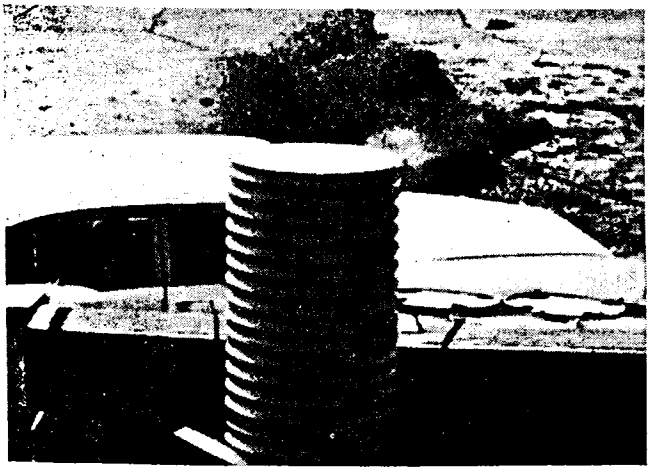

5

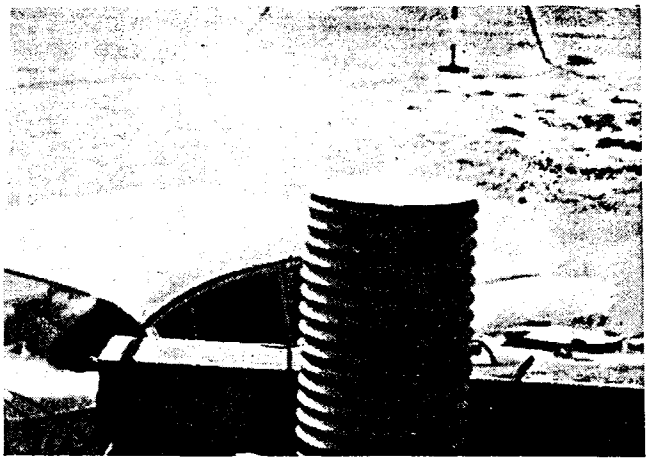

6

Figure 7. Sequence photographs of Test 1146-1.

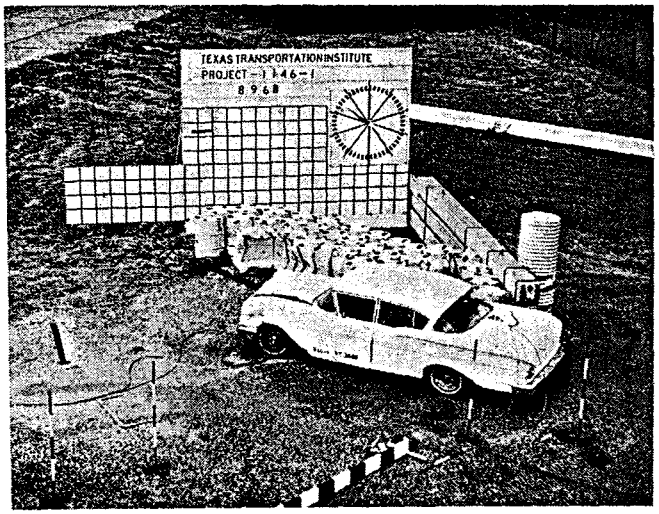

Figure 8. View of vehicle and impact area after test (1146-1).

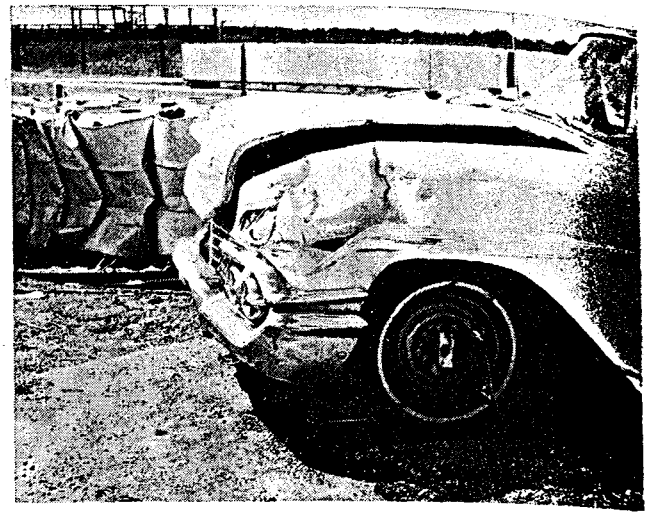

Figure 10. Vehicle after test (1146-1) showing damage area.

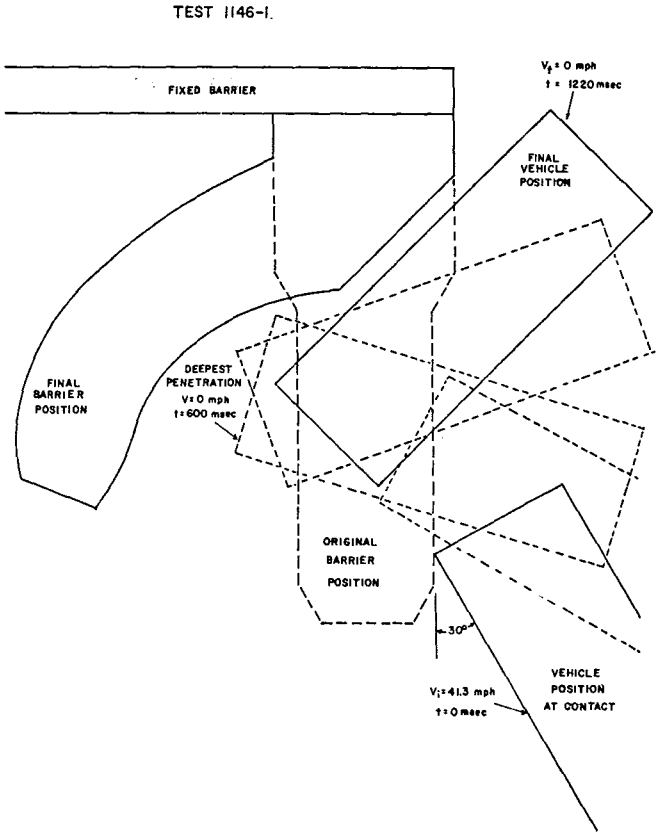

Figure 9. Position-time diagram, 1146-1.

Figure 11. Modular crash cushion after test (1146-1).

Test 1146-2

55-gallon drums with tops and bottoms cut, 3 rows four drums wide, 8 rows three drums wide, and 1 row two drums wide, surrounded by W-section guardrail, protecting rigid simulated bridge abutment (30° Test). See Figure 16.

Vehicle Weight = 3540 lbs (1957 Ford, 2-Door).

Vehicle Velocity = 49.9 mph or 73.2 fps.

Change in Velocity = 49.9 mph or 73.2 fps.

Average Deceleration = 6.3 g's (longitudinal).

Duration of Impact:

To Deepest Penetration = 360 ms.

To Final Vehicle Position = 1600 ms.

Stopping Distance (Longitudinal) = 13.2 ft.

Angular Movement While Stopping = 50°.

The crash cushion was modified in Test 1146-2 by surrounding the barrels with 12-gauge, W-section guardrail. This guardrail was free to slide through the supports at the bridge pier so that it could move with the barrels as they deformed under head-on impact (see Figure 16). It was anticipated that the guardrail would provide additional lateral stability for the crash cushion and, at low angles of impact, might redirect the vehicle. The test showed that additional lateral stability was provided by the guardrail; but at an impact angle of 30° the vehicle was not redirected. The vehicle pocketed in the cushion-guardrail system producing extensive damage to the left front of the vehicle. The average longitudinal deceleration was 6.3 g's which is still well within the human tolerance limit.[2] Damage to the vehicle consisted of deforming the left front approximately 18 inches; damaging the front bumper, bumper arms, hood, radiator, water pump, fender and frame; and blowing out the left front tire. This cushion-guardrail system did not perform as intended.

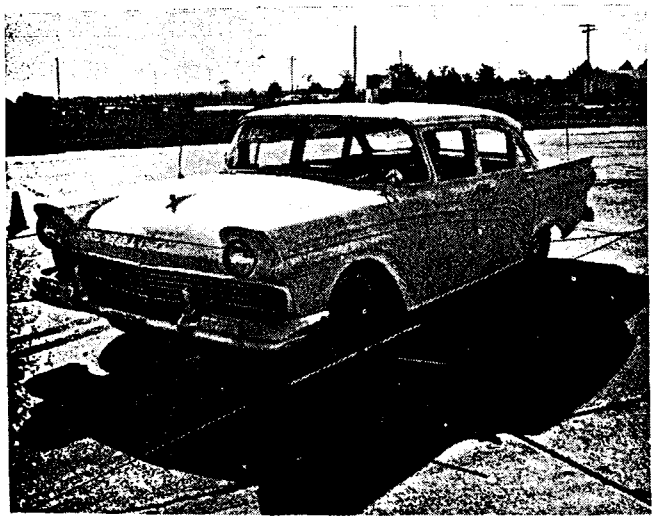

Figure 12. Vehicle before test (1145-2).

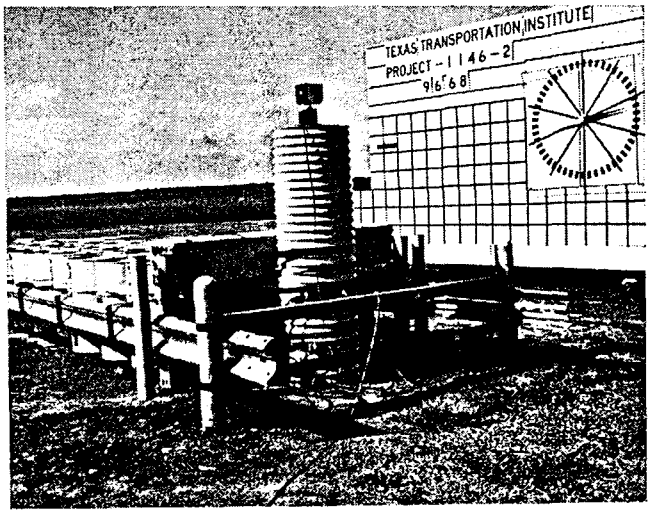

Figure 14. Rear view of modular crash cushion before test, W-section Guardrail is free to slip through supports as barrels deform (1145-2).

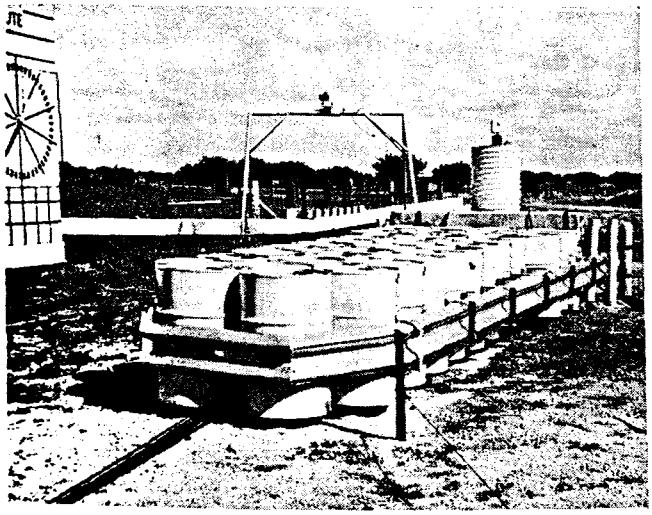

Figure 13. Modular crash cushion before test, installed in front of rigid barrier (1146-2).

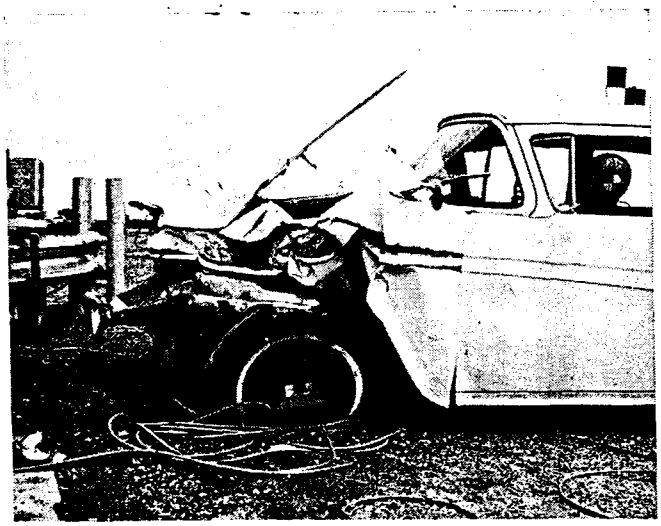

Figure 15. Vehicle after test (1146-2).

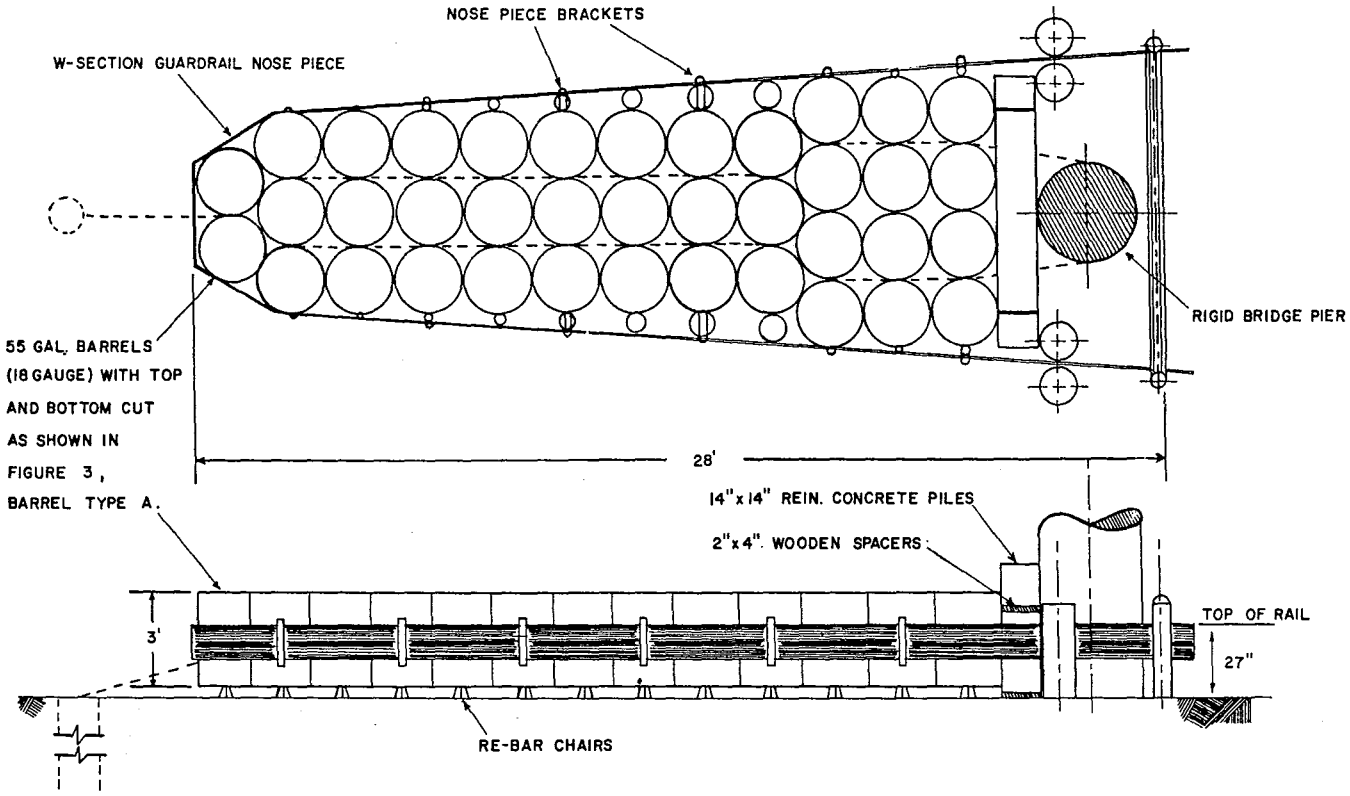

Figure 16. Modular crash cushion, Test 1146-2.

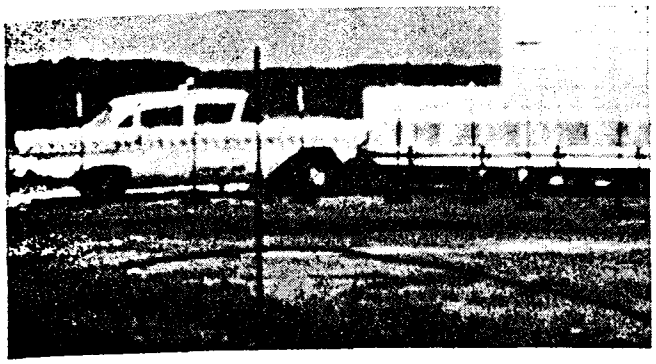

1a

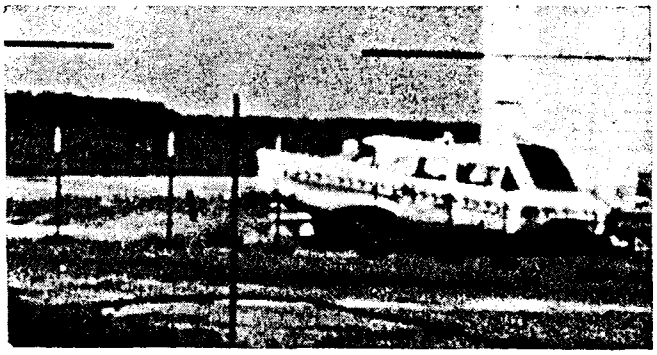

2a

3a

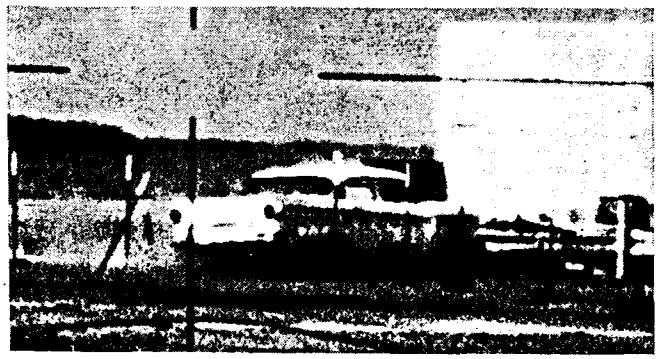

4a

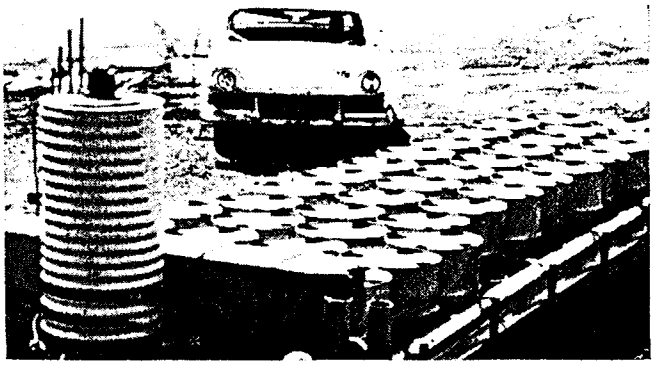

1b

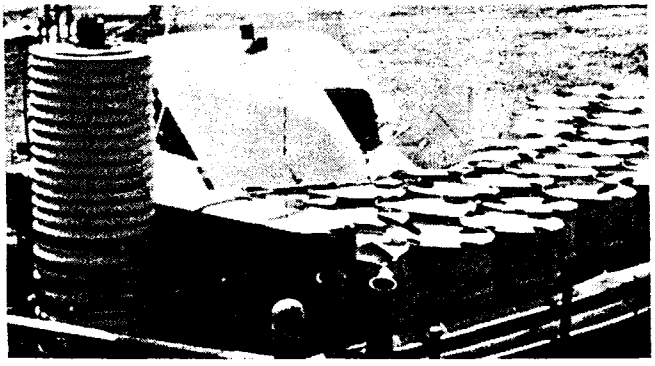

2b

Figure 17. Sequence photographs of Test 1146-2 (two views).

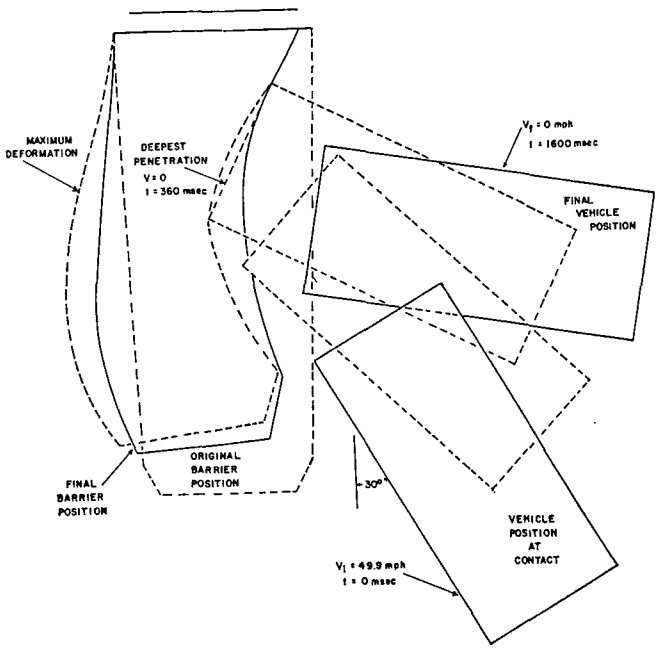

Figure 18. Position-time diagram, 1145-2.

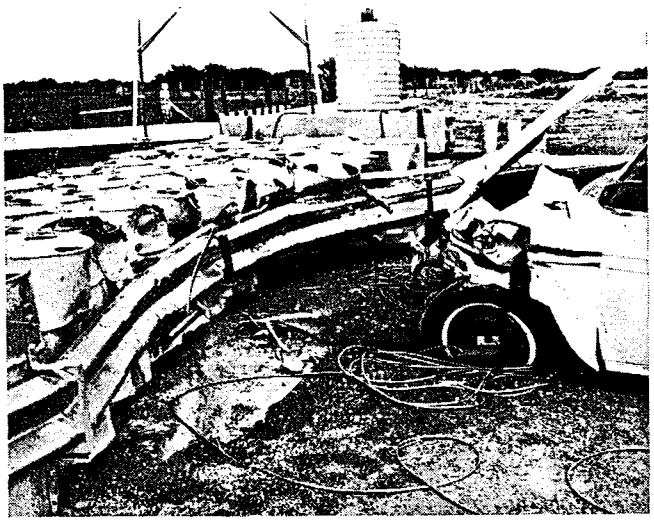

Figure 19. Impact side of modular crash cushion after test (1146-2).

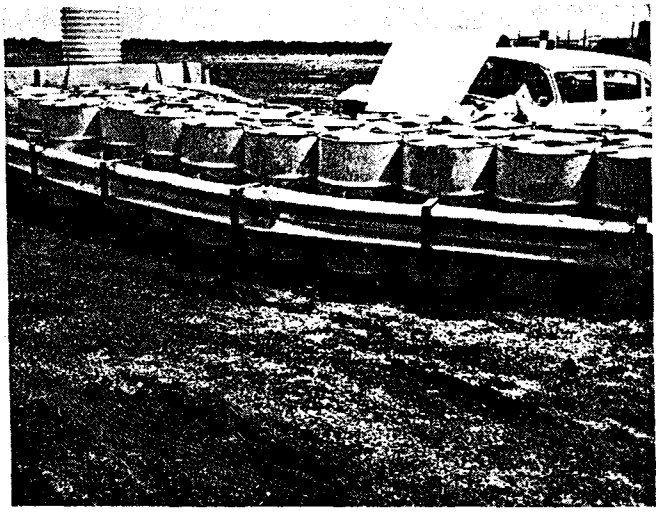

Figure 20. Opposite side of modular crash cushion after test (1146-2).

Test 1146-3

55-gallon drums with tops and bottoms cut, 3 rows four drums wide, 8 rows three drums wide and 1 row two drums wide, protecting rigid simulated bridge abutment (Head-on Test). See Figure 2.

Vehicle Weight = 4460 lbs (1957 Buick, 2-Door).

Vehicle Velocity = 55.7 mph or 81.7 fps.

Change in Velocity = 5 .7 mph or 81.7 fps.

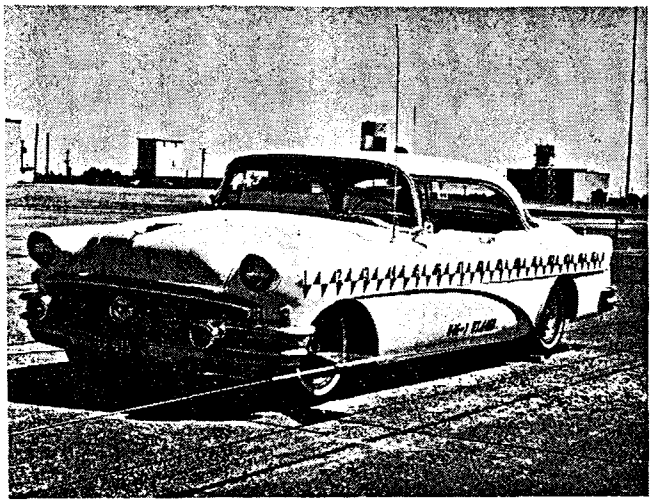

Figure 21. Vehicle before test (1146-3).

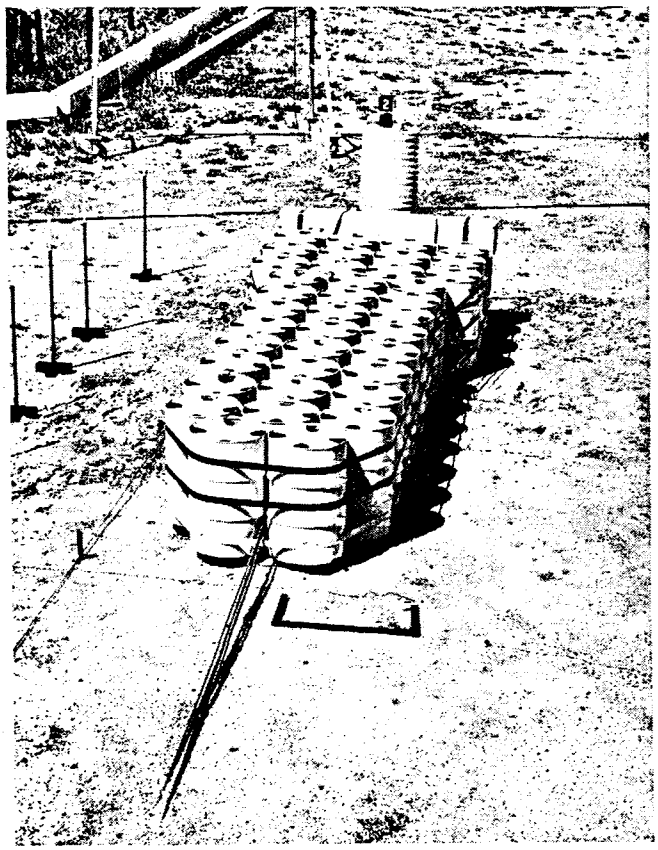

Figure 22. Modular crash cushion before test (1146-3).

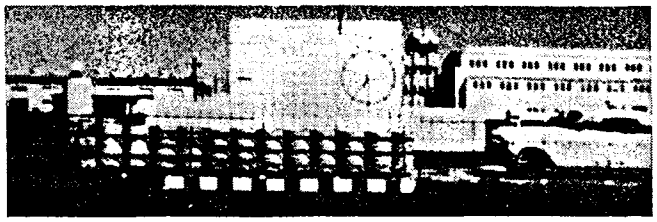

1

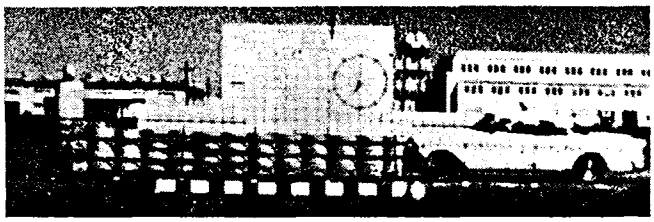

2

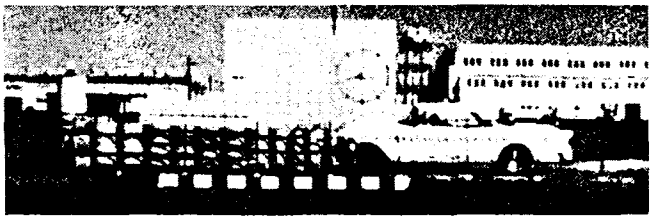

3

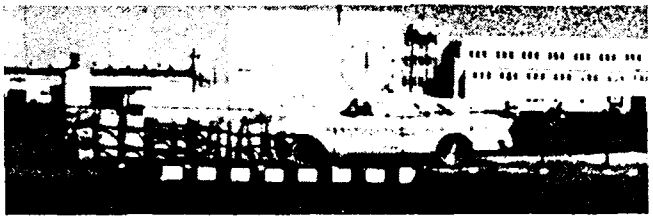

4

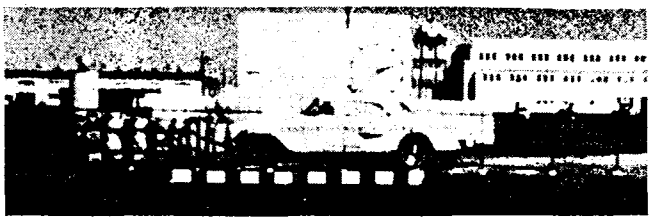

5

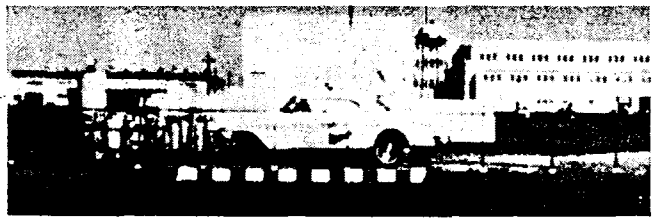

6

Figure 23. Sequence photographs of Test 1146-3.

Average Deceleration = 6.2 g's (longitudinal).
Duration of Impact:
To Deepest Penetration = 390 ms.
To Final Vehicle Position = 1000 ms.
Stopping Distance (Longitudinal) = 16.0 ft.
Angular Movement While Stopping = Negligible.

This test of the same barrel arrangement that was used in Test 1146-1 verified the performance of the system during head-on collisions. The car was stopped in a distance of 16 ft at an average deceleration of 6.2 g's. Damage to the car was superficial. There was minor damage to the front bumper, grill, hood, and radiator harness, and to the radiator and bumper arms.

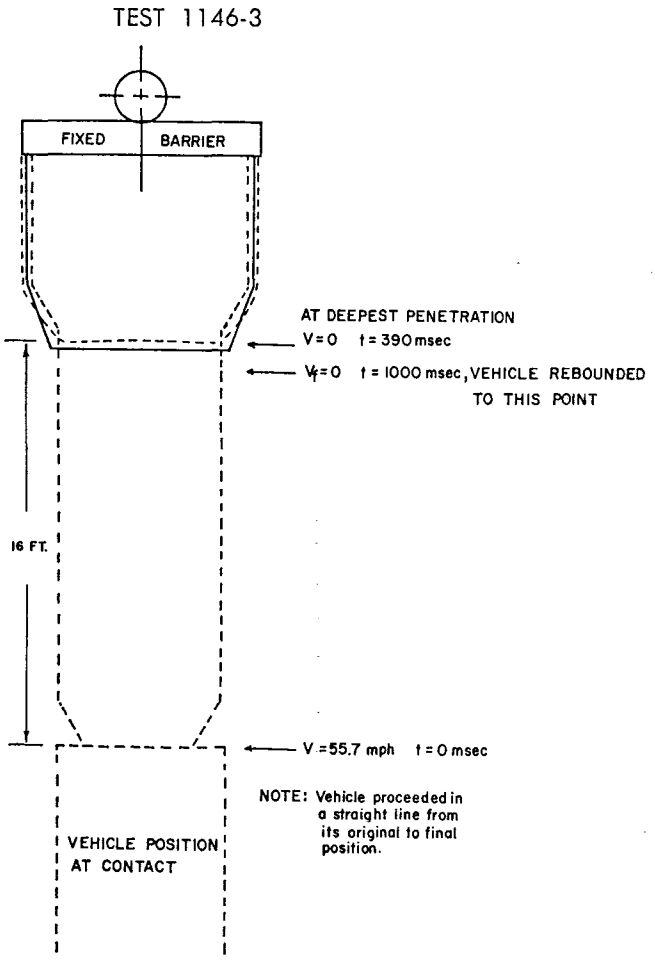

Figure 24. Position-time diagram, 1145-3.

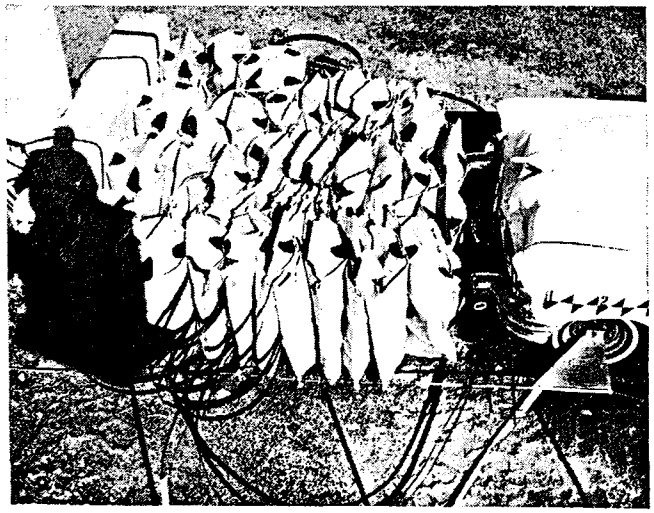

Figure 25. Modular crash cushion after test (1146-3).

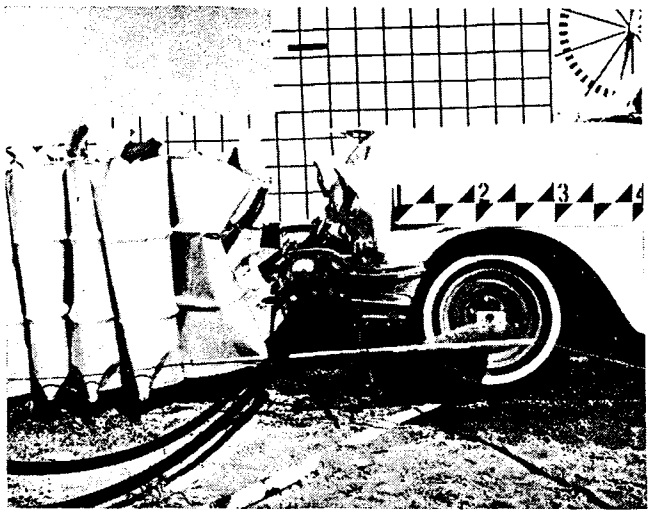

Figure 26. Almost negligible damage to vehicle (1146-3).

55-gallon drums with tops and bottoms cut, 3 rows four drums wide, 8 rows three drums wide and 1 row two drums wide, protecting rigid simulated bridge abutment (20° Test). See Figure 2.

Vehicle Weight = 3860 lbs (1957 Chevrolet, 4-Door).
Vehicle Velocity = 40.7 mph or 59.7 fps.
Change in Velocity = 40.7 mph or 59.7 fps.
Average Deceleration = 4.6 g's (longitudinal).
Duration of Impact:
To Deepest Pentration = 470 ms.
To Final Vehicle Position = 1700 ms.
Stopping Distance (Longitudinal) = 13.7 ft.
Angular Movement While Stopping = 81°.

The same barrel configuration that was used in Tests 1146-1 and -3 was also used for 1146-4. Adequate provision was made for anchorage of the cables and the impacting angle was reduced to 20°. The vehicle was brought to a halt in 13.7 feet at an average longitudinal deceleration of 4.6 g's. The only shortcoming of the protective barrier in this test was that significant strain energy was stored in the barrels and cables as the car was brought to a halt, which resulted in a rebound of the car back away from the barrier. Figure 31 shows the final position of the car. In the case of an actual test, the driver would probably have his foot on the brake during the collision which would eliminate this rebound. The barrel systems which have been installed have been provided with a crushable cable support at the bridge pier which should reduce the vehicle rebound significantly.

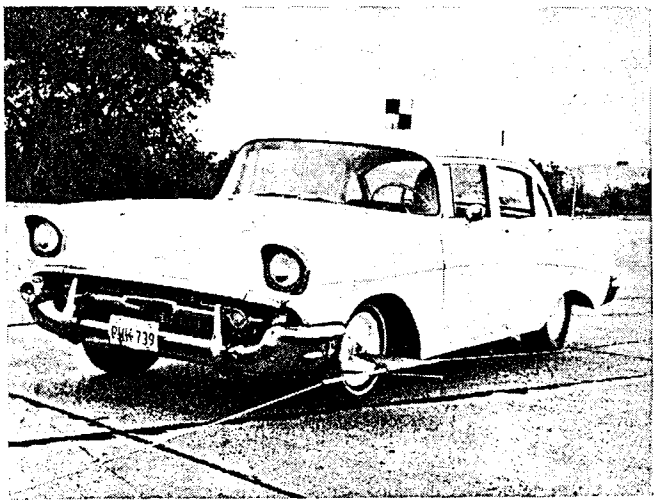

Figure 27. Vehicle before test (1146-4).

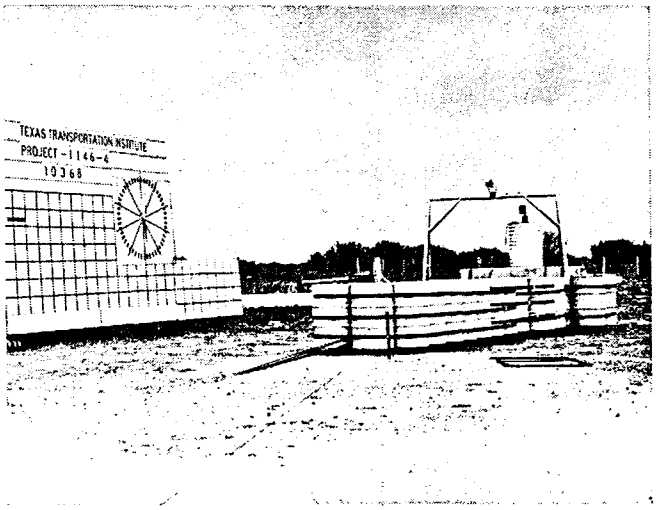

Figure 28. Modular crash cushion before test (1146-4).

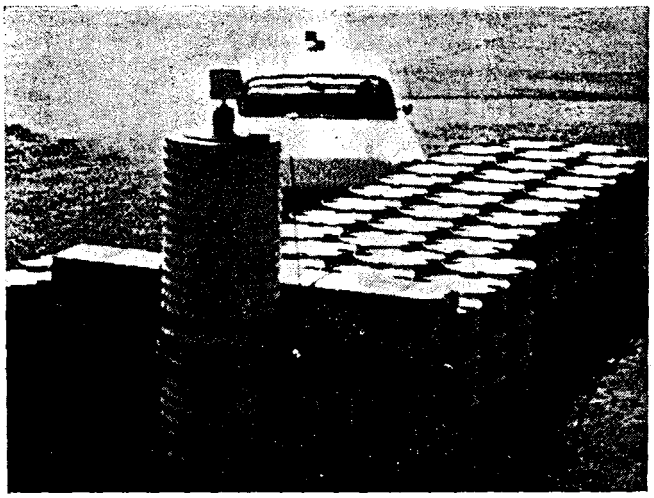

1

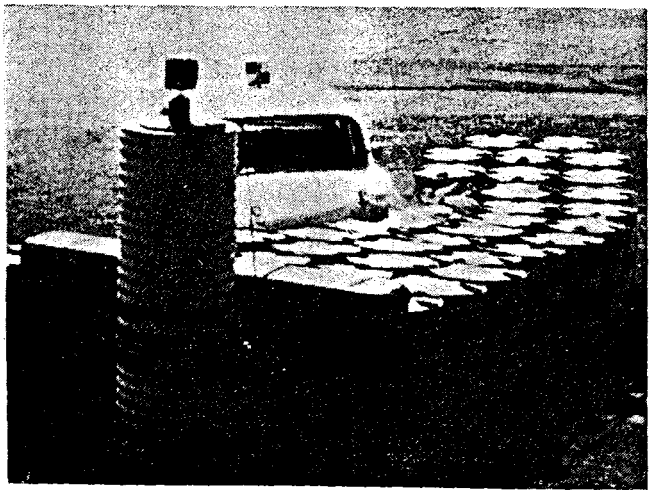

2

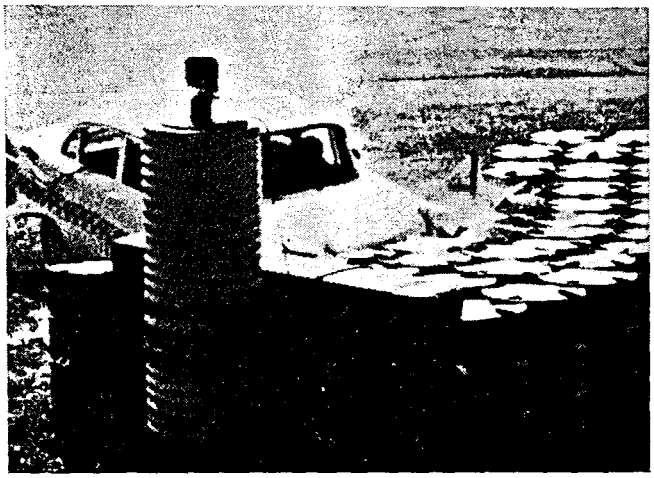

3

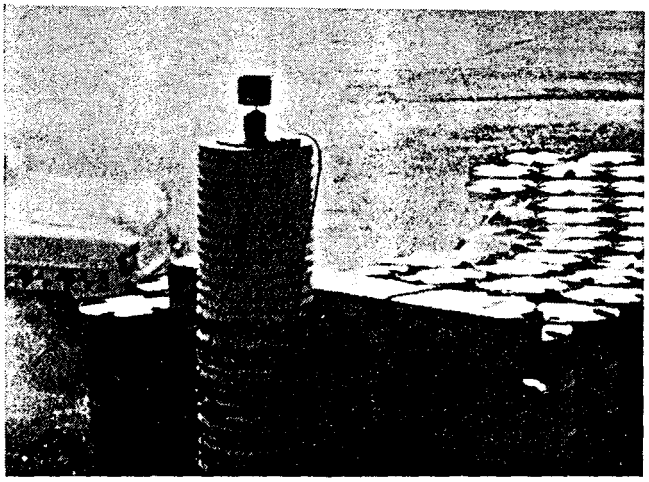

4

Figure 29. Sequence photographs of test (1146-4).

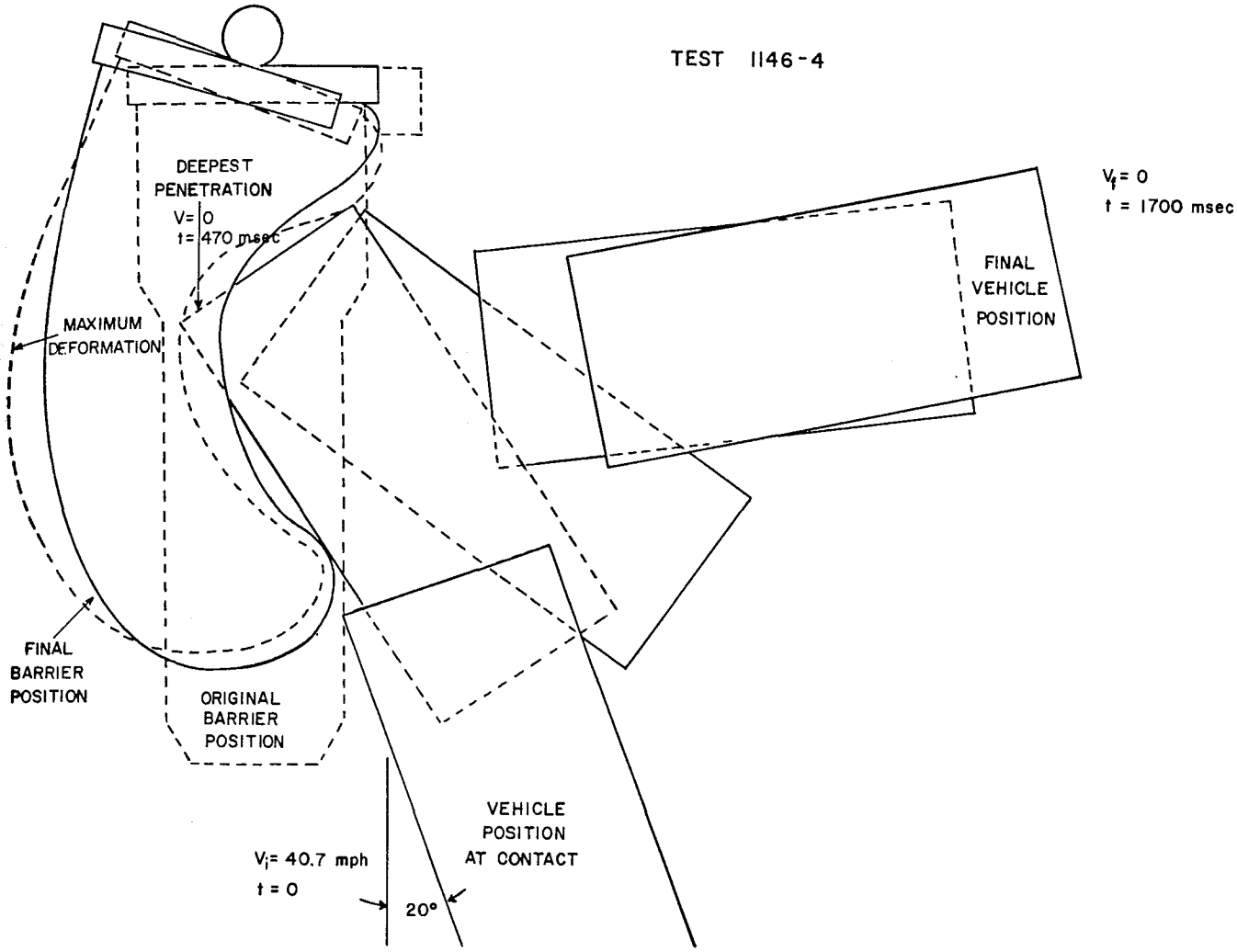

Figure 30. Position-time diagram, 1145-4.

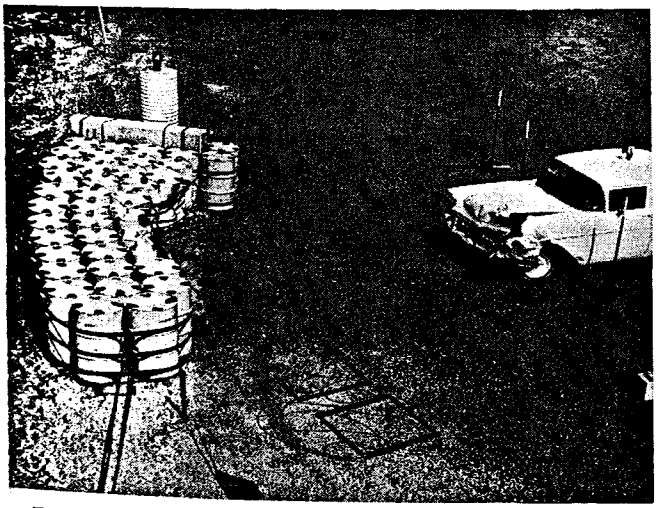

Figure 31. View of impact area after test (1146-4).

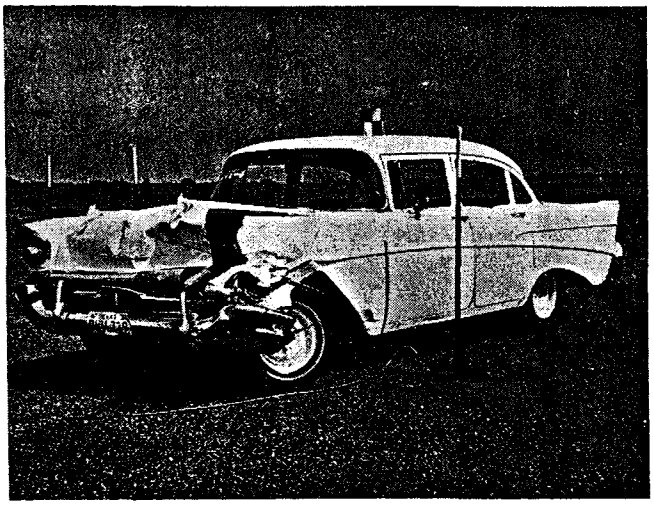

Figure 32. Vehicle after test (1146-4).

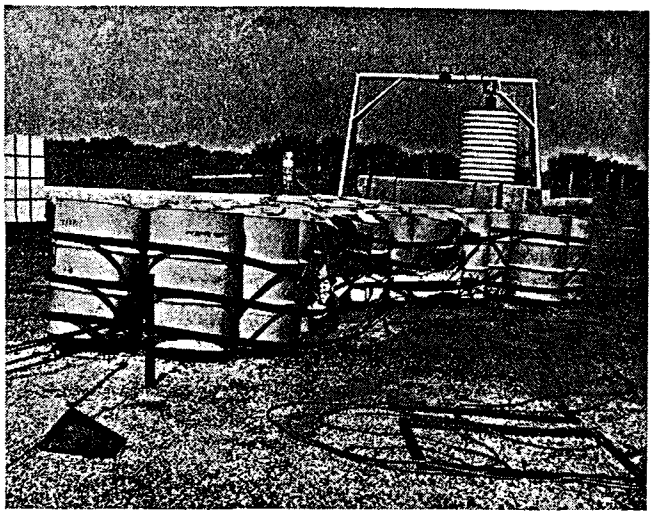

Figure 33. Modular crash cushion after test (1146-4).

Test 1146-5

55-gallon drums with tops and bottoms cut, 3 rows five drums wide, 5 rows four drums wide, 1 row three drums wide, and 1 row two drums wide, protecting rigid simulated bridge abutment (Head-On Test). See Figure 37.

Vehicle Weight = 3360 lbs (1961 Dodge, 4-Door).

Vehicle Velocity = 52.6 mph or 77.1 fps.

Change in Velocity = 52.6 mph or 77.1 fps.

Average Deceleration = 7.6 g's (longitudinal).

Duration of Impact:

To Deepest Penetration = 320 ms.

To Final Vehicle Position = 2200 ms.

Stopping Distance (Longitudinal) = 12.1 ft.

Angular Movement While Stopping = Negligible.

In some of the planned field applications, the necessary area for the configuration of barrels tested in Tests 1146-1 through -4 was not available. In order to accommodate these shorter locations, a slightly different barrel system was designed using a different arrangement of barrels. This new arrangement is shown in Figure 37. Test 1146-5 was a head-on collision with this modified system. The vehicle was stopped in 12 ft at an average deceleration level of 7.6 g's. Although this deceleration is slightly higher than that achieved with the protective system used in Test 1146-3, it is still well within the human tolerance limit.[2] This slightly higher deceleration level is also indicated by the slightly

Figure 34. Vehicle before test (1146-5).

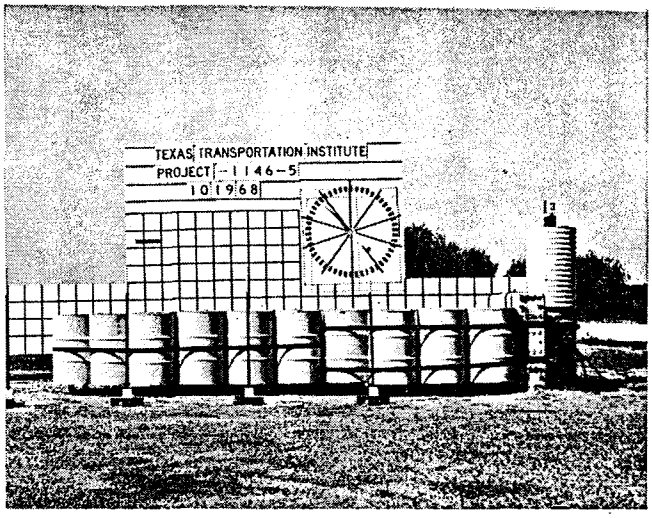

Figure 35. Modular crash cushion before test, side view (1146-5).

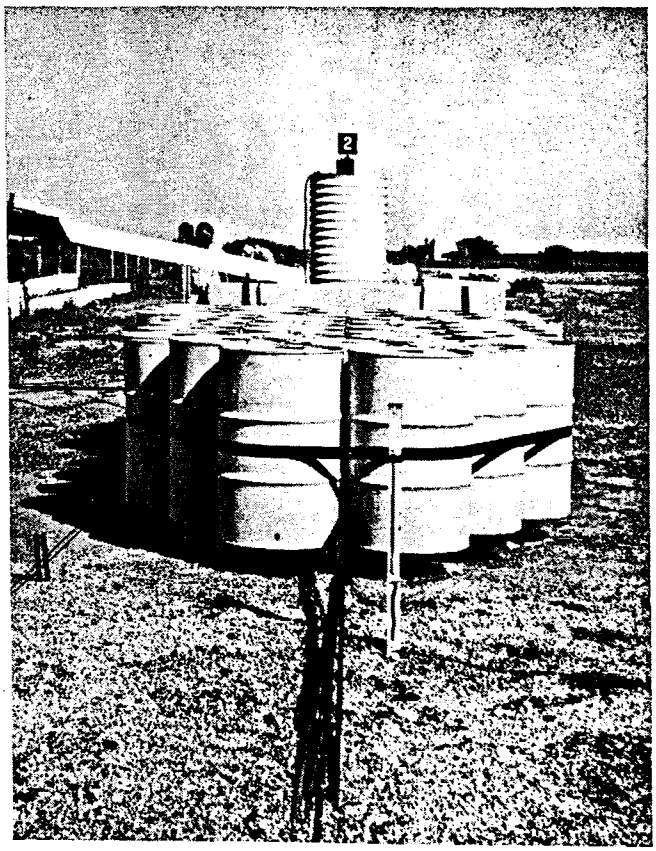

Figure 36. Front view of modular crash cushion before test (1146-5).

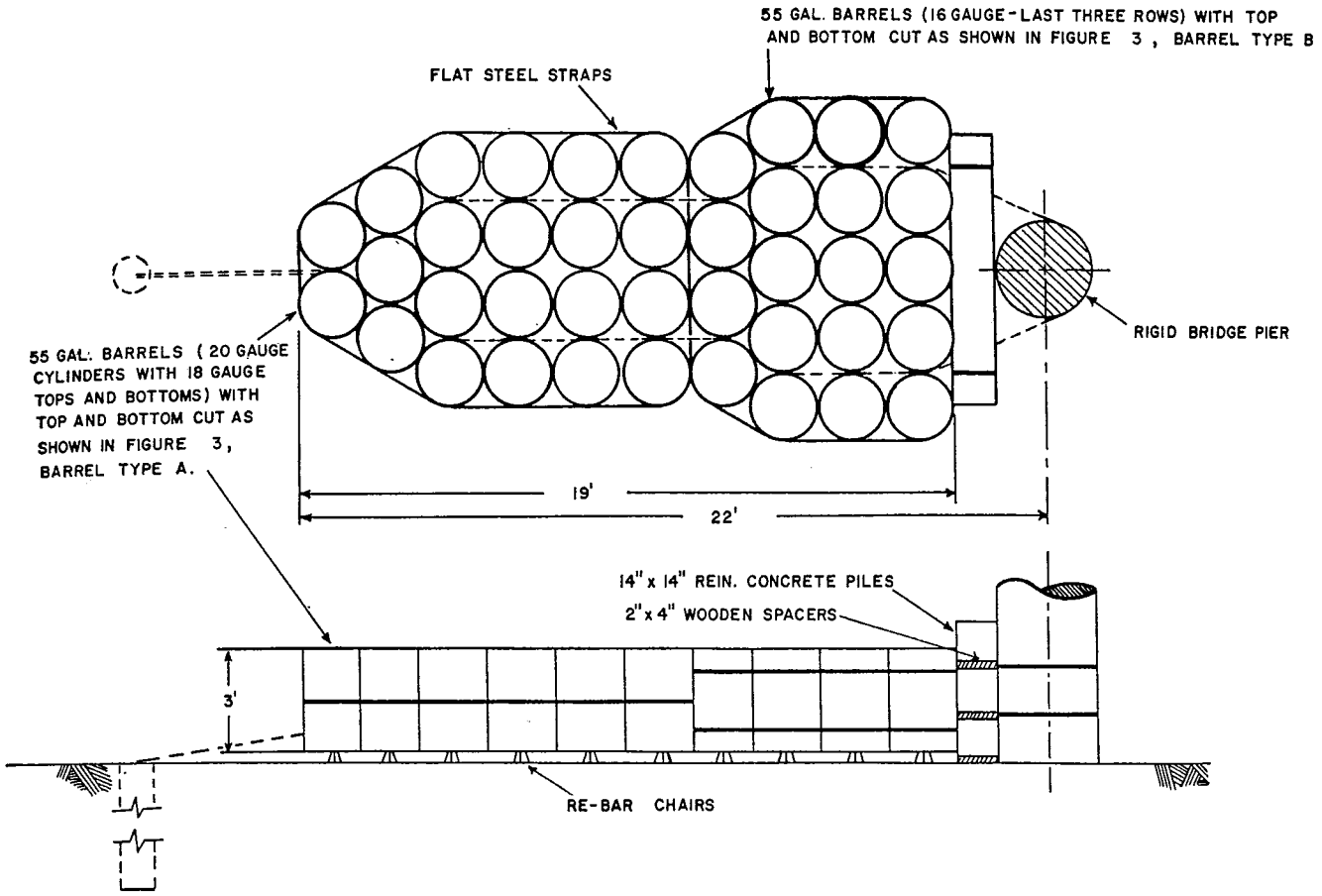

Figure 37. Modular crash cushion, Test 1146-5.

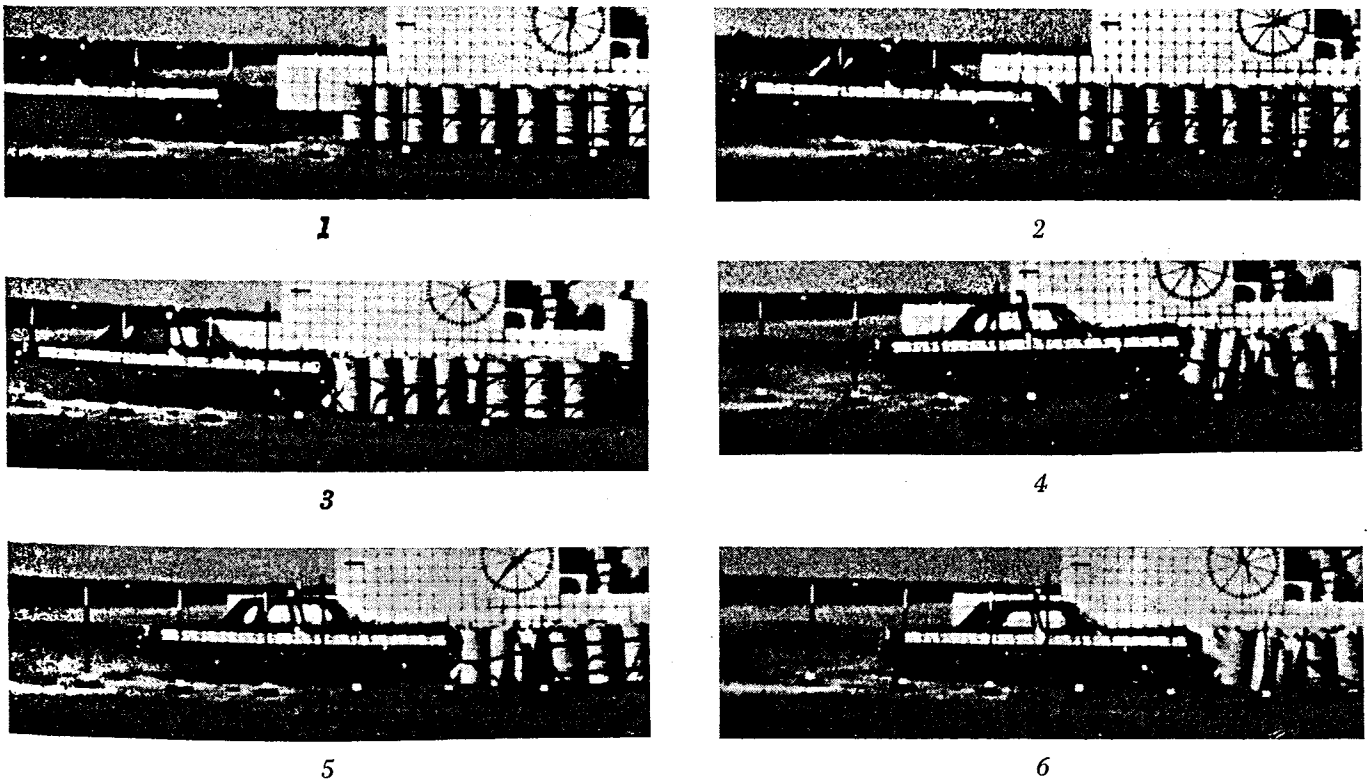

Figure 38. Sequence photographs of test (1146-5).

higher degree of damage to the front of the test vehicle. There was deformation of the entire front of the vehicle and damage to grill, hood, radiator, gravel shield, and headlight.

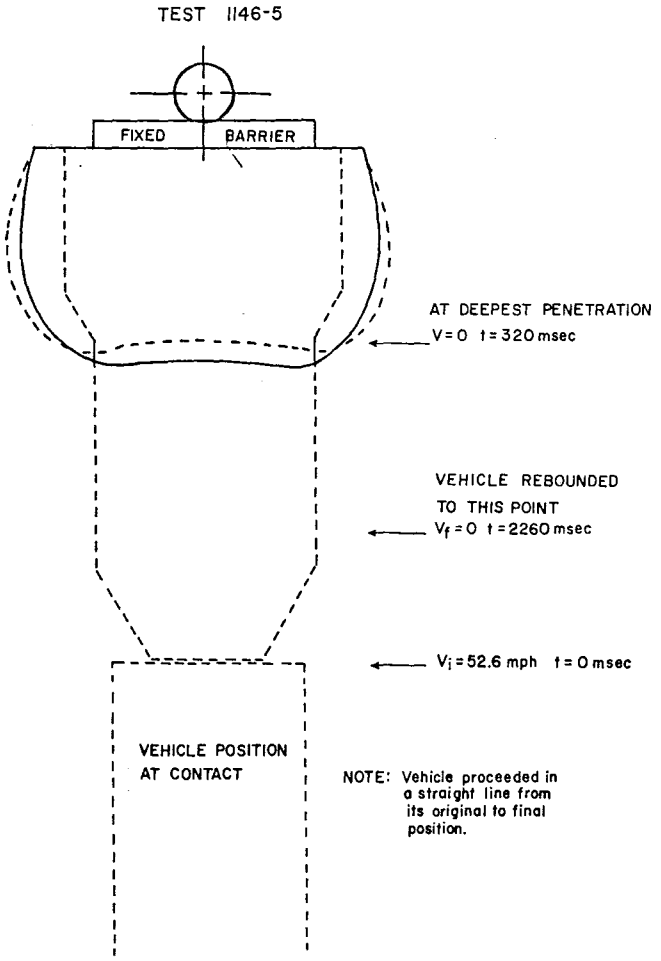

Figure 39. Position-time diagram, 1145-5.

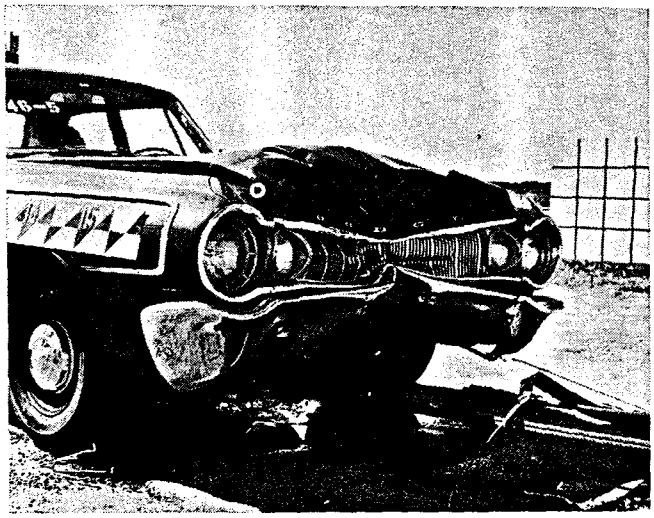

Figure 40. Damaged area of vehicle after test (1146-5).

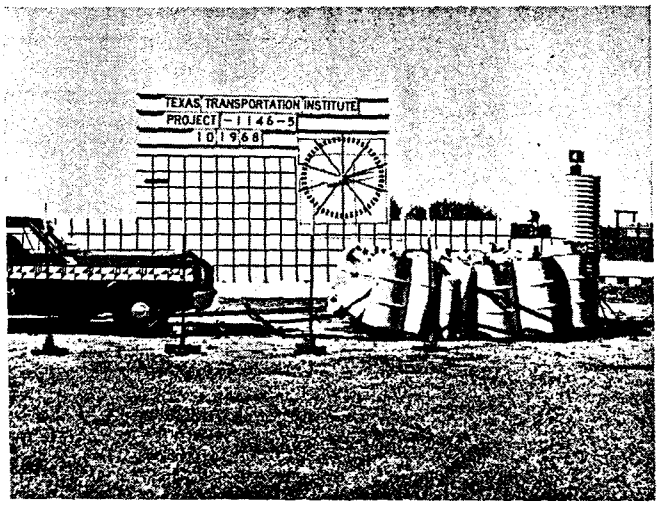

Figure 41. Impact area after test (1146-5).

Discussion of Complete Test Series

A comparison of the three angle vehicle crash tests is given by Table 1. Test 1146-1 gave the longest stopping distance and correspondingly the smallest values of vehicle decelerations. Undue emphasis should not be placed on this test because of the occurrence of a structural failure. When the vehicle collided with the barrels, the cable support which was in front of the nose of the barrel system was torn loose. This support can be seen emerging from the ground in Photographs 4 and 5 of Figure 7. The failure of this cable support allowed the Crash Cushion to rotate laterally away from the vehicle which produced a significantly smaller resistance to the movement of the vehicle. If the vehicle had been traveling at a higher speed (velocity at impact was 41 mph) the secondary impact of the vehicle with the bridge abutment could have been severe (see Photograph 6 of Figure 7).

In Test 1146-2 the Crash Cushion was surrounded with 12-gauge, W-section guardrail which was not rigidly attached to the barrels and could slip through the supports as the barrels crushed. It was intended that the guardrail would help provide the necessary lateral stability and redirect the vehicle. The necessary lateral stability was achieved, but at the high impact angle of 30° the vehicle pocketed in the barrel guardrail system. Due to the increased rigidity provided by the guardrail, the average deceleration level was higher than in either of the other two angle impact tests.

Another good comparison between the characteristics of the Modular Crash Cushion with and without the guardrail is in the damage to the test vehicles. Figures 15 and 19 show extensive damage to the test vehicle used in Test 1146-2, while the vehicle damage is rather

TABLE 1. ANGLE TESTS—SUMMARY OF DATA

Test Number	1146-1	1146-2	1146-4
Angle of Impact, Degrees	30	30	20
Stopping Distance (Longitudinal), ft	16.2	13.2	13.7
Vehicle Weight (W), lbs	3640	3540	3860
Vehicle Velocity (V), fps	60.6	73.2	59.7
Max. Deceleration (Longitudinal), g's	4.7[1]	6.8[1]	9.0[3]
Max. Acceleration (Transverse), g's		6.4[1]	7.4[1] 11.0[3]
Average Deceleration (Longitudinal), g's	2.5[1] 3.5[2]	3.9[1] 6.3[2]	4.0[2] 4.6[3]
Average Acceleration (Transverse), g's		0.8[1]	3.5[1] 6.4[3]

[1]Electronic Accelerometers.

[2]Calculated from Stopping Distance.*

[3]Impact-O-Graph.

*The most reliable deceleration measurement is the one calculated from the stopping distance and the vehicle initial velocity by the equation,

$$G_{avg} = \frac{v^2}{2gS},$$

Where

v = initial velocity in ft/sec,

S = movement of vehicle's center of gravity in ft from its position at first contact to its position when the vehicle has a longitudinal velocity of zero,

g = acceleration of gravity, 32.2 ft/sec.^{2}

nominal in Tests 1146-1 and 1146-4 (Figures 10 and 31).

The final test of an angular collision showed an acceptable interaction between the vehicle and the protective system. At an impact angle of 20° the vehicle was stopped with an average deceleration of 4.6 g's, a level which is not difficult for a *restrained* passenger to undergo. The only shortcoming of this test was the amount of elastic energy stored in the barrel and cable system which rebounded the vehicle out and away from the impact area after the crash. Provisions can be made to reduce this stored energy in the field installations by securing the cables with deformable supports.

In addition, two head-on tests, summarized in Table 2, were conducted as part of this study. Test 1146-3 stopped the test vehicle with an average deceleration of only 6.5 g's. The stopping distance was 15.95 ft. This test was conducted on the 23 ft 6 in. protective system. A shorter, more compact attenuator was used in test

TABLE 2. HEAD-ON TESTS—SUMMARY OF DATA

Test Number	1146-3	1146-5
Vehicle Weight (W), lbs	4460	3360
Vehicle Velocity (V), fps	81.7	77.1
Stopping Distance (D), ft	15.95	12.1
Max. Deceleration, g's (longitudinal)	8.0[1] 13.0[3]	12.0[3]
Avg. Deceleration, g's (longitudinal)	5.2[1] 6.5[2] 6.8[3]	7.6[2] 6.4[3]
Attenuation Index $AI_{(max)} = \frac{G\ (max.\ barrels)}{G\ (max.\ rigid)^4}$	0.27	0.25
$AI_{(avg)} = \frac{G\ (avg.\ barrels)}{G\ (avg.\ rigid)^4}$	0.22	0.26

[1]Electronic Accelerometer.

[2]Calculated from Stopping Distance.

[3]Impact-O-Graph.

[4]G. (max. rigid) = 0.9V*, G (avg. rigid) = 0.574V*, V in mph.

*Emori, Richard I., "Analytical Approach to Automobile Collisions," SAE Paper 680016, Engr. Congress, Detroit, January 8, 1968.

1146-5. This system stopped the test vehicle in only 12.1 ft with an average deceleration of 7.6 g's.

A comparison of the severity of these crashes is given in Table 2 by the Attenuation Index. The maximum and average decelerations which would have been experienced by the vehicle had it struck a rigid barrier, such as a concrete retaining wall, are calculated using the appropriate formula. These accelerations are divided into the maximum and average decelerations determined during the test. The result is the Attenuation Index. In these two tests the collision is approximately ¼ as severe as the collision would have been had the vehicle struck an unyielding object.

Another way of showing the satisfactory performance of these Crash Cushions is illustrated by Figure 42. This figure, which is based primarily on the work of Stapp and De Haven, defines the area of severe injury, area of moderate injury, and area of noninjury for human exposure to g levels of various durations. The tests of the barrel protective devices are shown by the large black dots. The numeral beside each dot designates the particular test. All barrel tests conducted by the Texas Transportation Institute are well within the area of acceptable human tolerance. It should be emphasized that this area was defined on the basis of a *restrained* passenger subjected to sternumward acceleration. Serious injury could result at these deceleration levels due to the "second collision" of the passenger with the interior of the car if the passenger is not restrained.

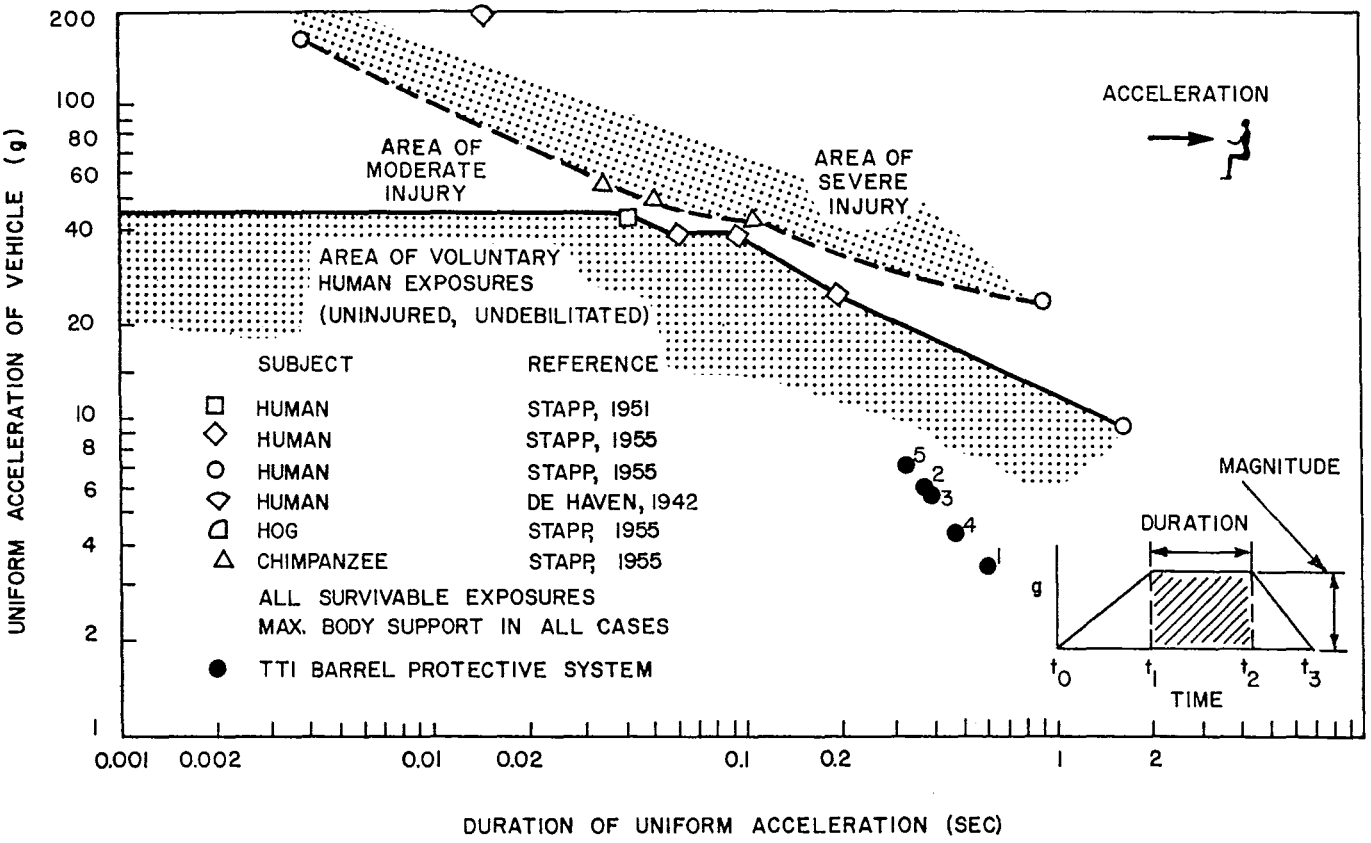

Figure 42. Maximum human tolerance limits to transverse acceleration (Sternumward G) (Eiband, 1959), Reference 2.

Design and Analysis

The following sections demonstrate the application of very simple principles of structural behavior to the design of Modular Crash Cushions and to the determination of the dynamic behavior of a speeding vehicle intercepting a Modular Crash Cushion.

Failure Mode

Figure 43 illustrates the assumed successive crushing of rows of barrels when the system is impacted head-on by a speeding vehicle. As the vehicle penetrates and deforms the Modular Crash Cushion, a stopping force is applied to the vehicle. In Figure 43-2 the first row of barrels has been crushed. Neglecting the inertia of the barrels, the force necessary to crush a single barrel, f_b, has been determined from laboratory static tests. Therefore, the force necessary to crush the first row of barrels (two abreast) will be two times f_b. Similarly, after the next eight rows of barrels have been crushed (at 3 x f_b), the total necessary crushing force will be four times f_b during the crushing of the last three rows (four abreast).

The crash tests have shown that the average deformation of each barrel, among those which are crushed, is 75% of its original diameter. Thus a barrel which was originally 24 inches in diameter can be expected to crush approximately 18 inches. By measuring the area under the static force-deformation curve for each particular type of barrel, the energy necessary to crush the barrel, e_s, can be determined. Figure 44 demonstrates this determination for the Type C barrels.

Analysis of full-scale vehicle crash test data, however, has indicated that the average energy consumed by each barrel in a Modular Crash Cushion, e_d, is actually about 50% higher than the static force-deformation curve indicates. Therefore, for design purposes, an energy consumption of 1.5 times the energy indicated by the simple static barrel tests should be used.

$$e_d = 1.5\ e_s.$$

There are several reasons this should be expected. (1) The actual distribution of forces on the barrels in the Crash Cushion is somewhat different from the force distribution on a single barrel during static laboratory tests. (2) The 2-inch welds which join the barrel rims at contact points contribute to the rigidity of the individual barrels. And (3), the interconnection of the barrels in the system contributes to the sum of the individual barrel strengths. By dividing this dynamic energy consumption per barrel by the deformation distance, 18 inches or 1.5 ft, the average dynamic crushing force

can be approximated. For barrel Type C this force would be:

$$\frac{e_d}{1.5 \text{ ft}} = \frac{1.5 \text{ (9 Kip-ft)}}{1.5 \text{ ft}} = 9 \text{ Kips.}$$

This determination of energy consumption per barrel, e_d, and dynamic crushing force, f_d, is the basic empirical information needed to develop the design procedure and to analyze proposed barrel arrangements for Modular Crash Cushions.

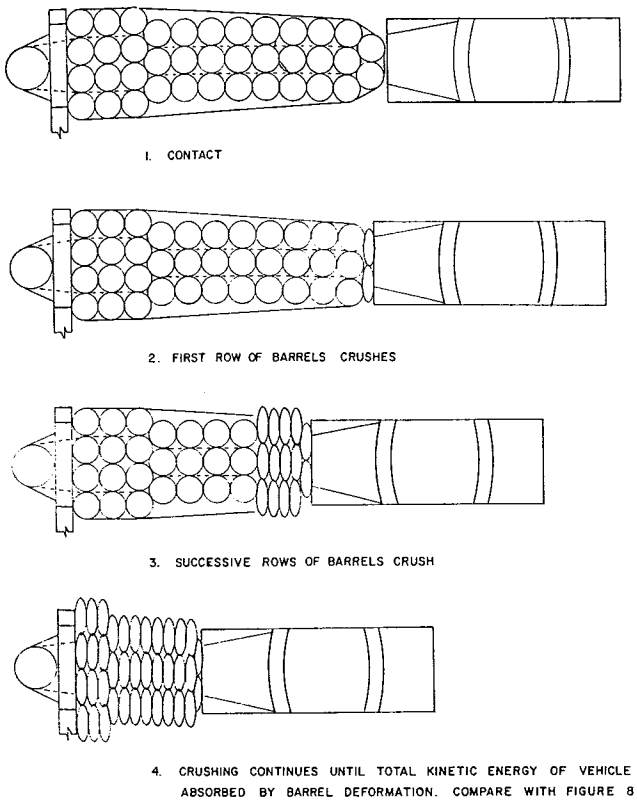

Figure 43. Sucessive crushing of modular crash cushion.

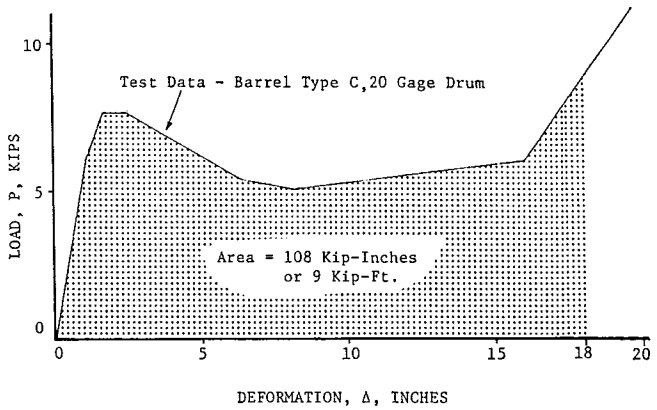

Figure 44. Single barrel force-deformation curve. (See Figure 45 for test set-up.)

Design Example

An impact attenuator must be placed at an elevated gore which will provide an acceptable deceleration level for a 4000-lb vehicle traveling 60 mph. Type C, 20-gage, 55-gallon steel drums with one 7-inch diameter hole in the center of each end are available for the construction of a Modular Crash Cushion.

The problem is to determine the arrangement of barrels that will fulfill these design criterion.

The vehicle kinetic energy is calculated by the following equation,

$$KE = \frac{1}{2} \frac{W}{g} V^2, \qquad (1)$$

Where

W is the design vehicle weight, 4000 lbs,

g is the acceleration of gravity, 32.2 ft/sec^2,

and V is the design vehicle velocity, 60 mph = 88 ft/sec.

Thus $KE = \frac{1}{2} \frac{4000}{32.2} (88)^2$

$= 480{,}000$ ft-lbs $= 480$ Kip-ft.

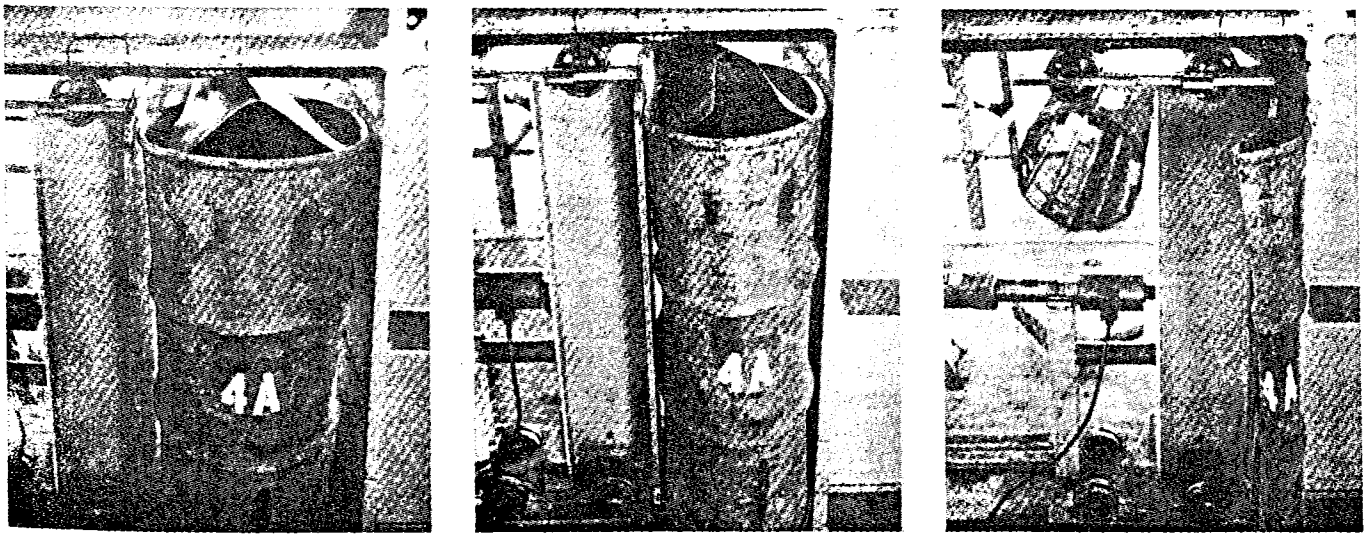

Deflection at 5 inches. *Deflection at 10 inches.* *Deflection at end.*

Figure 45. Failure mode of standard test.

If Type C barrels are used, it can be assumed that each barrel can absorb 13.5 Kip-ft (9 Kip-ft x 1.5) of energy. Therefore, the minimum number of barrels needed in the Crash Cushion is found by Equation 2.

$$N_b = \frac{KE}{e_d} = \frac{480 \text{ Kip-ft}}{13.5 \text{ Kip-ft/Barrel}} = 35.6 \text{ Barrels.} \quad (2)$$

Use $N_b = 36$ Barrels.

It now remains to arrange the barrels in such a way that an acceptable deceleration level will be achieved. If an average deceleration level, G_{avg}, of 6 g's is desired for the 4000-lb vehicle, the total length of the Crash Cushion can be found as follows:

Minimum stopping distance, L_s, is defined by:

$$L_s = \frac{V^2}{2g\ G_{avg}} = \frac{(88)^2}{2\ (32.2)\ 6} = 20 \text{ ft.} \quad (3)$$

Since the total length of the Crash Cushion, L_t, is defined by the crushing ratio (0.75) of individual barrels, the total barrier length must be:

$$L_t = \frac{L_s}{0.75} = \frac{20}{0.75} = 26.7 \text{ ft.} \quad (4)$$

Each barrel is two feet in diameter, so that the necessary number of rows of barrels, N_r, is:

$$N_r = \frac{26.7 \text{ ft}}{2 \text{ ft/barrel}} = 13.3 \text{ Barrels.}$$

Try 13 rows of barrels.
The number of barrels in each row, N_w, is:

$$N_w = \frac{N_b}{N_r} = \frac{36}{13} = 2.77.$$

Use 3 barrels in each row.

Thus the basic configuration would be as shown in Figure 46.

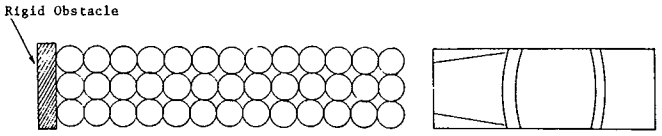

Figure 46. Nominal barrel arrangement.

A more desirable arrangement would be as shown by Figure 47. Placing a smaller number of barrels in the first few rows will decrease the crushing strength in these rows. This is compensated by the fact that when the velocity is high during crushing of the first few rows, the inertia force necessary to accelerate these barrels is highest. In contrast to this, placing more barrels in the last few rows increases the crushing strength in these rows. This is compensated by the fact that the vehicle has accumulated the mass of the preceding rows of barrels, thus decreasing the deceleration effect of this higher crushing strength. The result is a more constant deceleration force on the vehicle. This phenomenon will be explained further in the next section on analysis.

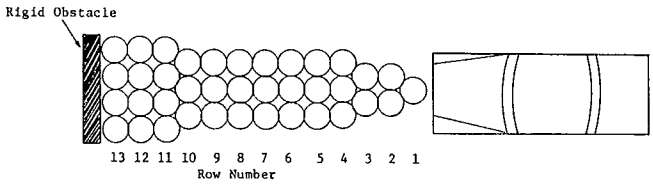

Figure 47. More desirable arrangement.

The stopping distance for any barrel arrangement can be found by determining the longitudinal dimension required by the number of barrels necessary to bring the design vehicle to a stop. In this case the number of barrels necessary, N_b, is 36. Counting from the front of the Crash Cushion shown in Figure 47, 36 barrels would be found in the first 12.5 rows of the barrier. The approximate stopping distance is then:

$$L'_s = 12.5 \text{ rows } (2 \text{ ft/row})\ 0.75 = 18.7 \text{ ft.}$$

Another way of determining stopping distance is by using a barrier crushing force (F_d) vs. vehicle penetration (L) diagram. This diagram is constructed for the total range of possible vehicle penetrations by multiplying the barrel crushing force, e_d, by the number of barrels in the row that is being crushed. This diagram is given in Figure 48 for the barrel configuration shown in Figure 47. The penetration necessary to dissipate the initial kinetic energy of the vehicle determines the stopping distance.

For example, a 2000-lb vehicle traveling 60 mph has a kinetic energy of

$$\frac{(2000)\ 88^2}{2\ (32.2)} = 240{,}000 \text{ ft-lbs} = 240 \text{ Kip-ft.}$$

The area under the curve, A_1, up to the vehicle stopping distance (max. vehicle penetration) must equal the vehicle initial kinetic energy. In this case, the stopping distance is 10.9 ft. Similarly, the area under the curve up to a penetration of 18.6 ft is equal to the kinetic energy of a 4000-lb vehicle traveling 60 mph. From these stopping distances, the average decelerations of 11 and 6.5 g's respectively can be calculated using Equation 3, i.e.

$$G_{avg} = \frac{V^2}{2g\ L_s}$$

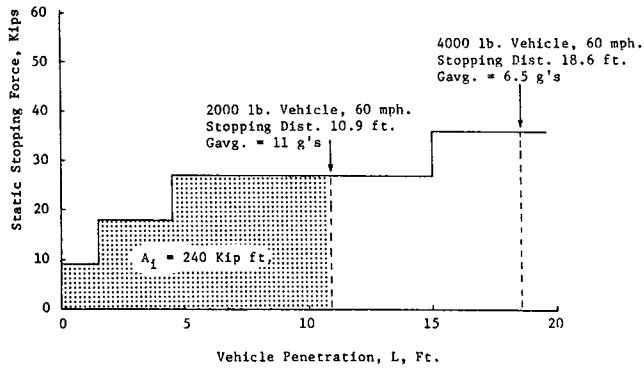

Figure 48. Stopping distance determination.

Analysis

The interaction of vehicle and Modular Crash Cushion has been programmed for the IBM 7094 using an adaptation of the one-dimensional wave equation. Although this is the most exact solution to the problem, and is available if needed, the simplified solution presented here has been found to give fairly accurate results.

Consider the vehicle-cushion system (Figure 49) after a number of rows of barrels have been crushed, and the vehicle still has some significant velocity, V_v.

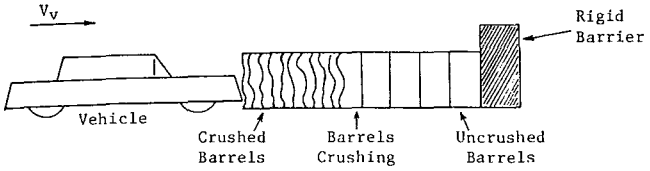

Figure 49. Interaction of vehicle-cushion system.

Free-body diagrams (in dynamic equilibrium) can be drawn for the various portions of the system as shown in Figure 50. The positive direction of each velocity, acceleration, or force is shown by the appropriate arrow.

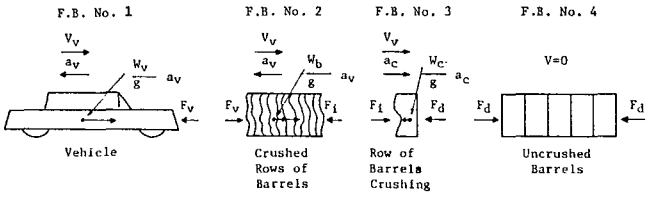

Figure 50. Free-body diagrams.

Where V_v = the velocity of the vehicle (at any time during crushing).

Note this is also the velocity of the barrels that have been crushed and are moving with the vehicle.

V_c = The velocity of the center of gravity (c.g.) of the row of barrels which is crushing.

a_v = The deceleration of the vehicle; also the deceleration of the crushed barrels.

a_c = The acceleration of the c.g. of the barrels which are crushing.

W_v = The weight of the vehicle.

W_b = The weight of the *crushed* barrels.

W_c = The weight of the barrels *which are crushing.*

F_v = The force at the vehicle-barrel interface.

F_i = The force at the *crushed barrels-crushing* interface.

F_d = The force at the crushing barrels-uncrushed barrels interface. This is taken to be the dynamic crush strength of the particular barrel row.

The following equilibrium equations can be written for these free bodies:

$$\text{F.B. No. 1} \quad F_v = \frac{W_v\, a_v}{g} \ .$$

$$\text{F.B. No. 2} \quad F_v = F_i - \frac{W_b}{g}\, a_v \ .$$

$$\text{F.B. No. 3} \quad F_i = \frac{W_c\, a_c}{g} + F_d \ .$$

F_i can be eliminated in these equations resulting in the following expression for F_v.

$$F_v = F_d - \frac{W_b\, a_v}{g} + \frac{W_c\, a_c}{g} \ . \qquad (5)$$

If acceptable approximations for a_v and a_c can be obtained, the force on the vehicle at any point during the test can be calculated. These values will be approximated as follows:

(1) a_v, the average vehicle deceleration, is approximated by a constant equal to $\frac{V^2}{2\,L_s}$ where

V = vehicle initial velocity and L_s is calculated from the force-penetration curve shown in Figure 48, or the other method previously discussed.

(2) Velocity, V_v, will be assumed to vary linearly with displacement from the initial velocity at contact to zero at maximum penetration.

(3) a_c is equal to $\frac{V_v^2}{2\,L'}$ where L' is the distance from the c.g. of the row of barrels which is crushing when crushing of the particular row starts, to the same c.g. when crushing of the particular row is finished (i.e. the next row of barrels starts to crush).

An inherent assumption in this treatment is that the rows of barrels crush in order (i.e., row 1, row 2, . . . row n) from the front of the barrier until the necessary energy has been dissipated. It is recognized that (1) and (2) are theoretically incompatible assumptions. It will be shown, however, that using these simplifying assumptions will still give a reasonably accurate description of the system behavior.

With these assumptions, the force on the vehicle, F_v, throughout the event can be calculated; and from F_v, the variation in deceleration throughout the event (in g's) can be calculated by the following equation:

$$g_v = \frac{F_v}{W_v} \qquad (6)$$

This analysis has been performed on the three head-on tests which have been carried out to date. The results are compared with the photographic data in Figure 51. This correspondence of the theory with the test data seems quite acceptable; especially when considering the wide variations in developing estimates of decelerations from photographic data. An example of the calculations necessary to apply the theory is given in the

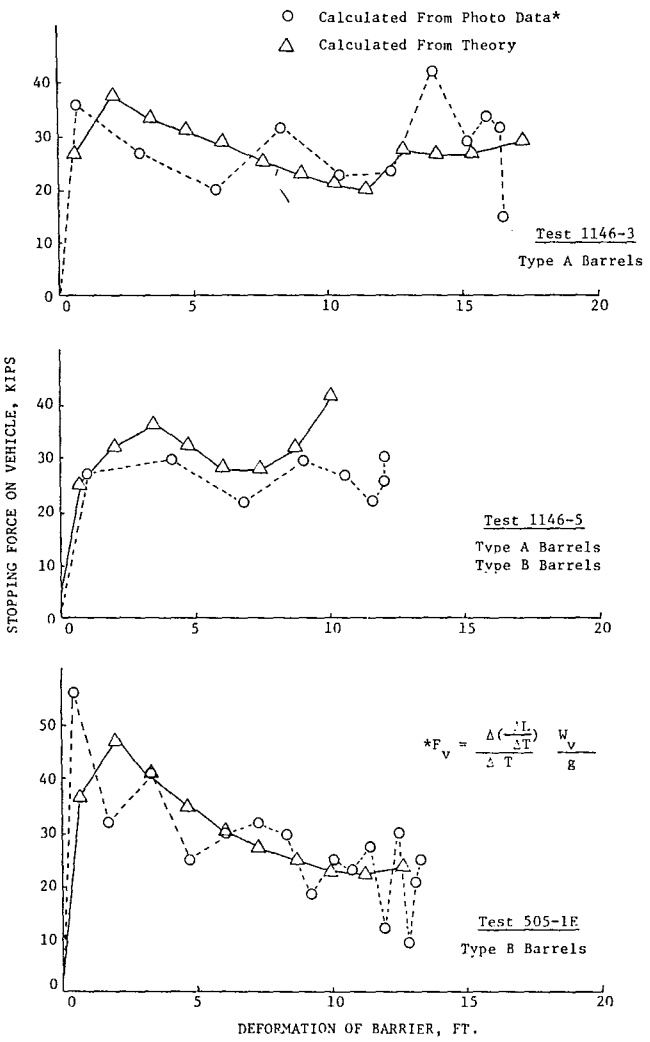

Figure 51. Comparison of theoretical with calculated stopping forces.

Appendix for the barrel configuration shown in Figure 47.

The unique characteristic of this vehicle crash attenuation system can be shown by considering Equation 5. The term $\frac{W_b}{g} a_v$ is the mass of the barrels which have accumulated on the front of the vehicle and are decelerating at the same rate as the vehicle. This mass times the deceleration, a_v, has the effect of decreasing the total force on the vehicle, as shown by the negative sign in Equation 5. All other systems tested or proposed to date (with the exception of the "Dragnet" which has a negligible mass) do not have this advantage, but must either pick up the total mass of the impact attenuator at the time of initial contact or completely dissipate the finite areas of resistance which are encountered.

Thus, this "accumulation of barrel mass" by the vehicle has the effect of decreasing the total force on the vehicle; especially toward the end of a vehicle-cushion interaction when this mass becomes relatively large. The other term in Equation 5, $\frac{W_c a_c}{g}$, has its most pronounced effect on vehicle stopping force at the beginning of the vehicle-cushion interaction when vehicle velocity is high, resulting in a high acceleration rate necessary to get a row of crushing barrels moving at the same velocity as the vehicle.

Thus it is in the interest of a more uniform vehicle stopping force to put a minimum number of barrels in the first few rows when the $\frac{W_c a_c}{g}$ term is most influential, and more barrels in the last few rows when the $\frac{W_b a_v}{g}$ term is working toward decreasing the stopping force.

Conclusions

The Modular Crash Cushion is an effective vehicle crash attenuation device for both head-on and angular collisions. All tests show deceleration rates well within the tolerance limits of restrained humans.

The extreme economy of this system as compared to other proposed systems is apparent. The cost of individual barrels delivered from the factory will range from $6 to $7. Used barrels can be purchased for as little as $2. The Modular crash cushion can be fabricated and installed by semiskilled laborers. The system should be painted with a rust-preventive and should be inspected periodically so that extensive rusting does not greatly alter the crushing strength of the barrels. The total cost for materials and fabrication of this type of system should range from $300 to $600 depending on whether new or used barrels are available. The cost of installing the barrel system will be highly variable depending on whether freeway modifications are necessary to accommodate the system or whether the freeway was originally built to include these systems.

Replacement should be relatively easy after a barrel system is struck by a vehicle. It may prove feasible to replace the entire system with a spare system which could be stored in a highway department maintenance yard. This could be accomplished quickly during a low density traffic period. The system which was struck could then be repaired by maintenance personnel if elements of it are still usable.

Selected References

1. Hirsch, T. J., "Barrel Protective Barrier," Technical Memorandum 505-1, Texas Transportation Institute, Texas A&M Research Foundation, a progress memorandom On Contract No. CPR 11-5851, U. S. Department of Transportation, Federal Highway Administration, Bureau of Public Roads, June 17, 1968.
2. Damon, Albert; Stoudt, Howard W.; and McFarland, Ross A., *The Human Body in Equipment Design*, Harvard University Press, Cambridge, Massachusetts, 1966.

Appendix

Calculation of Force-Displacement Curve

For the Design Example on Page 21, Confirguation of Figure 47. (See Analysis, page 23.)

V_i = initial vehicle velocity = 88 ft/sec.

W = weight of vehicle = 4000 lbs.

g = acceleration due to gravity = 32.2 ft/sec.^{2}

KE = initial vehicle kinetic energy = 480 kip-ft.

Barrel Type C (6000 pound static crush strength; 1.5 ft crush distance; barrel weight = 35 pounds).

STEP 1

Calculate the *dynamic* crush strength of the Modular Crash Cushion, F_d, as a function of deformation. (A plot of Force vs Displacement is helpful.)

— — — — — — — —

Dynamic crush strength per barrel = (1.5) (Static crush strength per barrel) = 9 kips per barrel

Location	*Deformation (ft)*	*F_d (kips)*
First Barrel	0 - 1.5	9
Second and Third row	1.5 - 4.5	18
Fourth thru Tenth rows	4.5 - 15.0	27
Eleventh thru 14th rows	15.0 - 21.0	36

STEP 2

Determine theoretical stopping distance from Force-Deformation calculations and initial kinetic energy of the vehicle. See Figure 48.

— — — — — — — —

Area under curve up to 15.0 ft. deformation
= [(1.5) (9.0) + (3.0) (18) + (10.5) (27)] kip-ft
= 351 kip-ft.

Energy remaining at 15.0 ft = (480 - 351) kip-ft = 129 kip-ft.

Additional deformation needed

$$= \left[\frac{129 \text{ kip-ft}}{36 \text{ kips}}\right] = 3.6 \text{ ft.}$$

L_s = Stopping Distance = (15.0 + 3.6) ft
$\simeq$ 18.6 ft.

STEP 3

Calculate the force required to accelerate the row of barrels being crushed, $\frac{W_c\ a_c}{g}$, assuming that the vehicle's velocity decreases linearly with deformation of the barrier.

— — — — — — — —

The change in velocity with displacement is:

$$\frac{\Delta V}{\Delta L} = \frac{88}{18.6} \text{ ft/sec/ft} = 4.73 \text{ ft/sec/ft.}$$

The velocity at any point is approximated by $V_v = V_i - (4.7)(L)$, where L is the deformation to that point.

The average force necessary to accelerate each row of barrels must be estimated. This average force will be plotted at the *mid-point* of crush of each row of barrels.

$$\frac{W_c\ a_c}{g} = \frac{W_c}{g}\frac{V^2_v}{2L'}$$

$$= \frac{(\text{No. of barrels in row being crushed})\ (0.035)\ (V_i - 4.7\ L)^2}{(32.2)\ (2)\ (0.75)}$$

$$= (\text{No. of barrels in row being crushed})\ (0.000725)\ (88 - 4.7\ L)^2.$$

The barrel weight is 0.035 kips. L is the deformation at the end of crush of the row being considered. This force is the *average* force for that row, and should be applied at the mid-point of crush. Let L_A = average deformation of the cushion during the crushing of a particular row of barrels. L' = the distance from the barrel c.g. when crushing starts, to the barrel c.g. when crushing stops. This distance can be shown to be 9 in. or 0.75 ft for 24 in. diameter steel barrels.

L, ft	L_A, ft	No. of barrels being accelerated	$\frac{W_c\ a_c}{g}$, kips
1.5	0.75	1	4.75
3.0	2.25	2	7.92
4.5	3.75	2	6.48
6.0	5.25	3	7.78
7.5	6.75	3	6.05
9.0	8.25	3	4.54
10.5	9.75	3	3.25
12.0	11.25	3	2.17
13.5	12.75	3	1.31
15.0	14.25	3	0.67
16.5	15.75	4	0.32
18.0	17.25	4	0.03

STEP 4

Calculate the force required to decelerate the crushed barrels moving with the vehicle, $\frac{W_b\ a_v}{g}$.

— — — — — — — —

This force is assumed to act at the c.g. of the rows of barrels which have been crushed.

$$\frac{W_b\ a_v}{g} = \frac{\text{(No. of barrels crushed) (0.035)}}{32.2}\ \frac{V_i^2}{2L_s}$$

$$= \frac{\text{(No. of barrels crushed) (0.035) (88)}^2}{(32.2)\ (2)\ (18.6)}$$

$$= (0.224)\ \text{(No. of barrels crushed)}.$$

Force applied at (ft)	No. of barrels decelerating	$\frac{W_b\ a_v}{g}$
2.25	1	0.22
3.75	3	0.67
5.25	5	1.12
6.75	8	1.79
8.25	11	2.46
9.75	14	3.14
11.25	17	3.81
12.75	20	4.48
14.25	23	5.15
15.75	26	5.82
17.25	30	6.72

STEP 5

Calculate the total force on the vehicle, F_v, as an incremental function of vehicle penetration into the barrier.

$$F_v = F_d - \frac{W_b\ a_v}{g} + \frac{W_c\ a_c}{g}\ .$$

Barrel Row	L_A, ft	F_d	$- \frac{W_b\ a_v}{g}$	$+ \frac{W_c\ a_c}{g}$	$= F_v$ (kips)
1	0.75	9	0	4.75	13.8
2	2.25	18	0.22	7.92	25.7
3	3.75	18	0.67	6.48	23.8
4	5.25	27	1.12	7.78	33.7
5	6.75	27	1.79	6.05	31.3
6	8.25	27	2.46	4.54	29.1
7	9.75	27	3.14	3.25	27.1
8	11.25	27	3.81	2.17	25.4
9	12.75	27	4.48	1.31	23.9
10	14.25	27	5.15	0.67	22.5
11	15.75	36	5.82	0.32	30.5
12	17.25	36	6.72	0.03	29.3

Plot F_v, vehicle stopping force, against L, the barrier deformation. A plot of the vehicle stopping force and static crush force vs. the barrier deformation for the design example is shown in Figure A1.

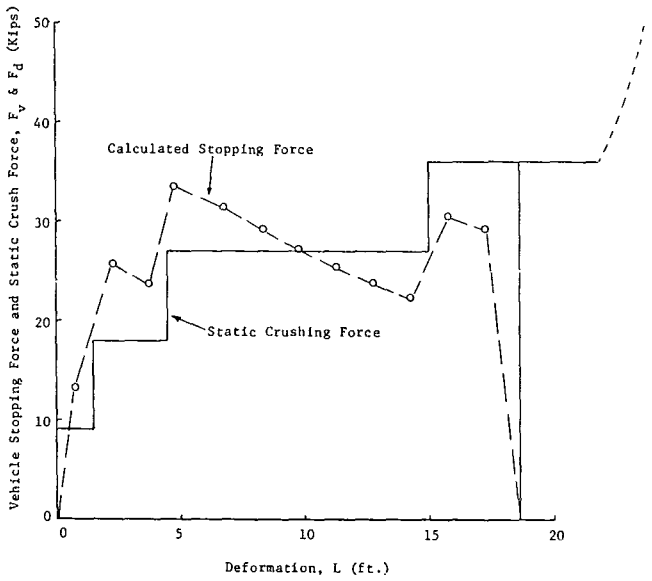

Figure A1. Vehicle stopping force and static crush force vs. barrier deformation for design example.

Speed Correlations

TABLE A1. SPEED CORRELATIONS ON 1146 SERIES

	Clock Speed rpm	Film #1 Speed fr.p.s.	Film #2 Speed fr.p.s.	V_i Switches ft/sec	V_i Film ft/sec	V_i Average ft/sec	mph
1146-1	1680*	503[H]	510[H]	59.7	61.5	60.6	41.3
1146-2	1680*	501[H]	500[H]	72.8	73.5	73.2	49.9
1146-3	1666	502[H]	498[H]	81.8	81.6	81.7	55.7
1146-4	1640	564[F]	496[H]	60.5	58.9	59.7	40.7
1146-5	1680*	510[H]			77.1	77.1	52.6

*Clock speed is based on 28 readings:
Average = 28 rps.
Standard Deviation = .46 rps.

High-Speed Film Data

TABLE A2. HIGH-SPEED FILM DATA
TEST 1146-1

	Time Milliseconds	Displacement ft	Velocity ft/sec
	0	0	
			63.0
	20.0	1.26	
			60.0
Impact	*40.0	*2.46	
			58.0
	60.0	3.62	
			57.2
	120.0	7.05	
			50.8
	180.0	10.10	
			45.0
	240.0	12.80	
			36.7
	300.0	15.00	
			28.0
	360.0	16.68	
			19.3
	420.0	17.84	
			27.7
	480.0	19.50	
			26.2
	540.0	21.07	
			27.0
	600.0	22.69	
			29.2
	660.0	24.44	
			27.7
	720.0	26.10	
			25.0
	780.0	27.60	
			24.0
	840.0	29.04	
			22.8
	900.0	30.41	
			20.5
	960.0	31.64	
			16.3
	1020.0	32.62	
			13.3
	1080.0	33.42	
			11.2
	1140.0	34.09	
			7.7
	1200.0	34.55	
			1.8
	1260.0	34.66	

tracking vehicle c.g. ↑ ↓ tracking vehicle rear

TABLE A3. HIGH-SPEED FILM DATA
TEST 1146-2

	Time Milliseconds	Displacement ft	Velocity ft/sec
	0	0	
			74.0
	30.0	2.22	
			72.5
	50.0	3.67	
			72.5
Impact	*70.0	*5.12	
			73.3
	100.0	7.32	
			66.6
	180.0	12.65	
			53.1
	260.0	16.90	
			36.2
	340.0	19.80	
			11.4
	420.0	20.71	
			−3.2
	500.0	20.45	
			−4.6
	580.0	20.08	
			−5.6
	660.0	19.63	
			−7.0
	740.0	19.07	
			−5.7
	820.0	18.61	
			−4.1
	900.0	18.28	
			−1.1
	980.0	18.19	
			−0.6
	1050.0	18.15	
			−0.3
	1140.0	18.12	
			−2.1
	1220.0	17.95	
			−1.4
	1300.0	17.84	
			−1.9
	1380.0	17.69	
			−2.1
	1470.0	17.52	
			−2.2
	1570.0	17.34	
			−0.2
	1670.0	17.32	

tracking vehicle c.g. ↑ ↓ tracking vehicle rear

TABLE A4. HIGH-SPEED FILM DATA
TEST 1146-3

	Time Milliseconds	Displacement ft	Velocity ft/sec
	0	0	
			82.7
	20.08	1.66	
			78.7
Impact	40.16	3.24	
			83.2
	*60.24	*4.91	
			76.4
	100.40	7.98	
			68.7
	140.56	10.74	
			63.0
	180.72	13.27	
			54.0
	220.88	15.44	
			47.5
	261.04	17.35	
			40.8
	301.20	18.99	
			28.6
	341.36	20.14	
			20.4
	381.52	20.96	
			10.7
	421.68	21.39	
			1.7
	461.84	21.48	
			−2.5
	502.00	21.38	
			−6.7
	542.16	21.09	
			−3.2
	582.32	20.96	
			−4.7
	622.48	20.77	
			−4.0
	662.64	20.61	
			−4.0
	702.80	20.45	
			−5.5
	742.96	20.23	
			−1.7
	783.12	20.16	
			−3.2
	823.28	20.03	

TABLE A5. HIGH-SPEED FILM DATA
TEST 1146-4

	Time Milliseconds	Displacement ft	Velocity ft/sec
	0	0	
			58.3
	50.40	2.94	
			59.5
Impact	*100.80	*5.94	
↑			54.7
↓ tracking vehicle c.g.	161.28	9.25	
			50.8
	221.76	12.32	
			41.7
	282.24	14.84	
			34.4
	342.72	16.92	
			19.8
	403.20	18.12	
			8.9
	463.68	18.66	
			5.3
	521.16	18.98	
			4.5
	584.64	19.25	
			2.0
	645.12	19.37	
			1.0
	705.60	19.43	
			−3.1
	806.40	19.24	
			−1.0
	907.20	19.18	
			−2.5
	1008.00	19.03	
			+0.2
	1108.80	19.04	
			−1.5
	1209.60	18.95	
			−3.1
	1310.40	18.76	
			−7.3
	1411.20	18.32	
			−5.6
	1512.00	17.98	
			−8.4
	1612.80	17.47	
			−7.3
	1713.60	17.03	
			−6.5
	1814.40	16.64	

↓ tracking vehicle rear ↑

TABLE A6. HIGH-SPEED FILM DATA
TEST 1146-5

	Time Miliseconds	Displacement ft	Velocity ft/sec
	0	0	
			76.6
	39.16	3.00	
			77.6
Impact	*78.32	*6.04	
			69.6
	137.06	10.13	
			55.8
	186.01	12.86	
			45.8
	234.96	15.10	
			32.1
	283.91	16.67	
			19.8
	332.86	17.64	
			9.8
	381.81	18.12	
			1.5
	401.39	18.15	
			−4.1
	420.97	18.07	
			−5.1
	440.55	17.97	
			−5.6
	460.13	17.86	
			−9.2
	479.71	17.68	
			−6.3
	577.61	17.06	
			−6.1
	675.51	16.46	
			−5.4
	773.41	15.93	
			−4.7
	871.31	15.47	
			−4.7
	969.21	15.01	
			−4.1
	1067.11	14.61	
			−3.8
	1165.01	14.24	
			−3.7
	1556.61	12.80	
			−2.9
	1948.21	11.68	
			−1.7
	2339.81	11.02	

Electronic Accelerometer Data

The following schematic diagrams show the circuit arrangement that was used in recording and filtering the electronic accelerometer data. The possibility exists that some nonlinearity was present in this system during the period in which these tests were conducted. For this reason, the accuracy of these data is not known. They should, therefore, be interpreted in a qualitative way only.

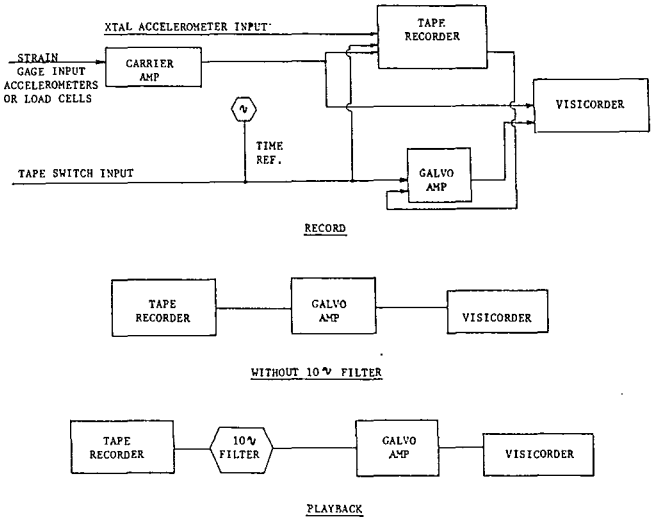

Figure A2. Circuit Diagrams.

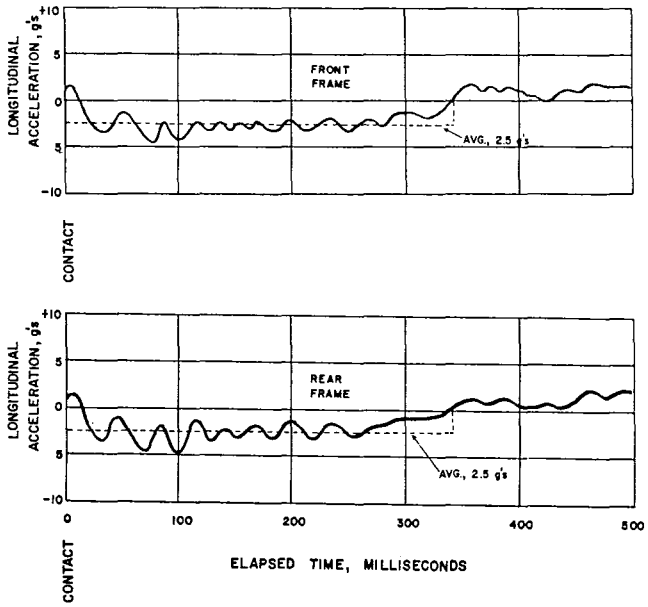

Figure A3. Test 1146-1, frame accelerometers.

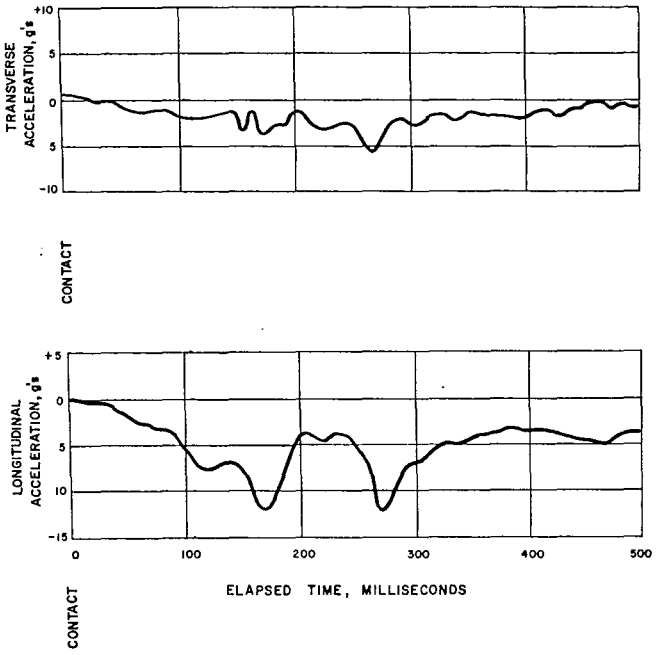

Figure A4. Test 1146-1, dummy accelerometer data.

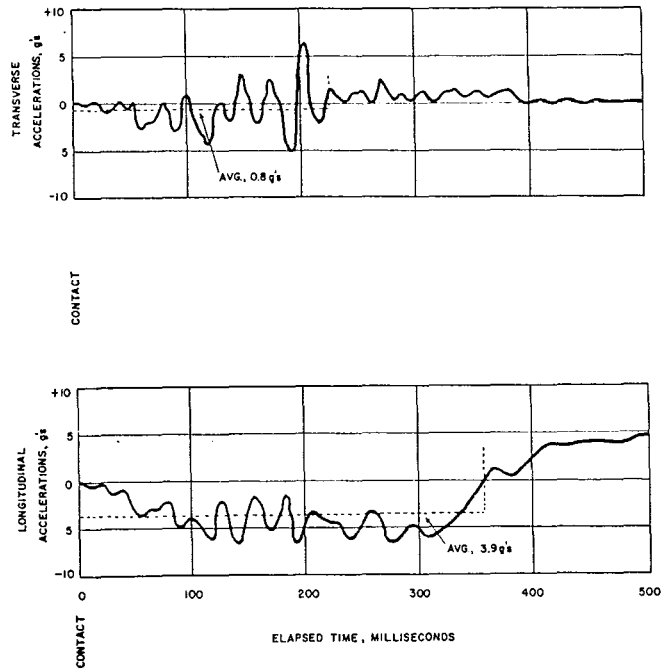

Figure A5. Test 1146-2, frame accelerometers.

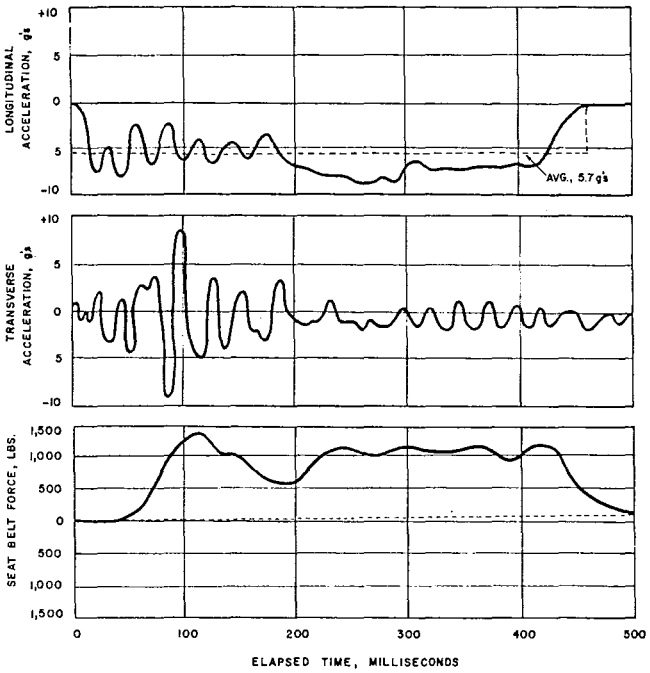

Figure A6. Test 1146-3 frame accelerometers and seat belt force.

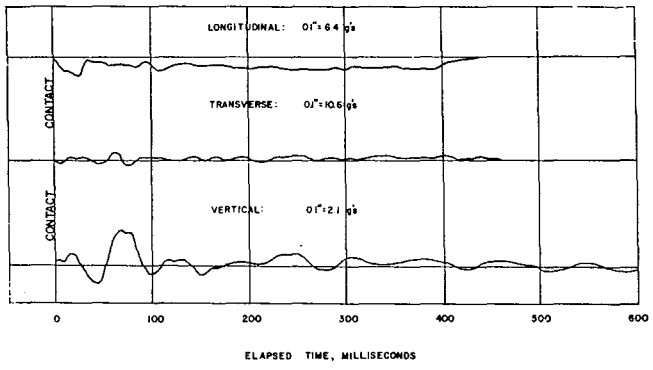

Figure A7. Impact-o-graph acceleration records, Test 1146-3.

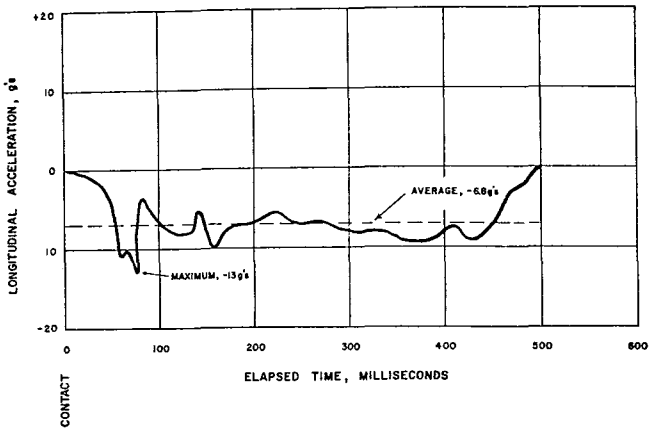

Figure A8. Enlargement of longitudinal impact-o-graph, Test 1146-3.

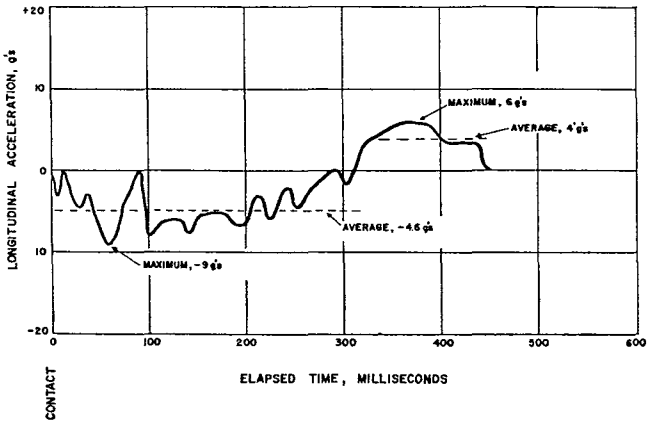

Figure A11. Enlargement of longitudinal impact-o-graph, Test 1146-4.

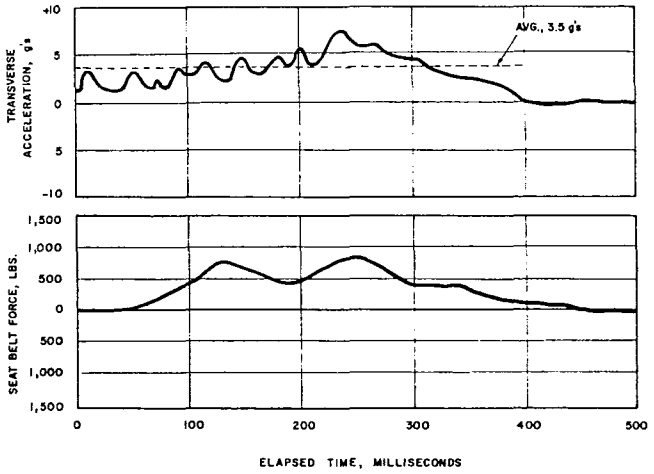

Figure A9. Test 1146-4 frame accelerometers and seat belt force.

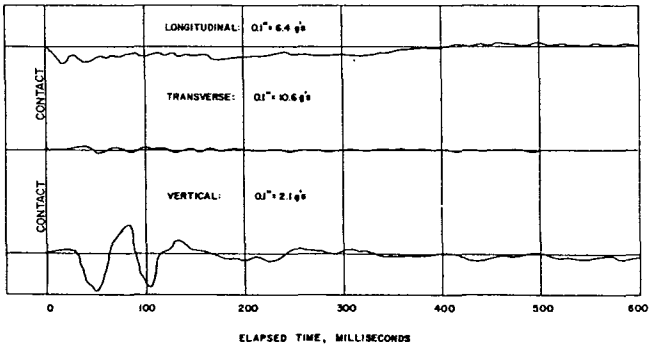

Figure A12. Impact-o-graph acceleration records, Test 1146-5.

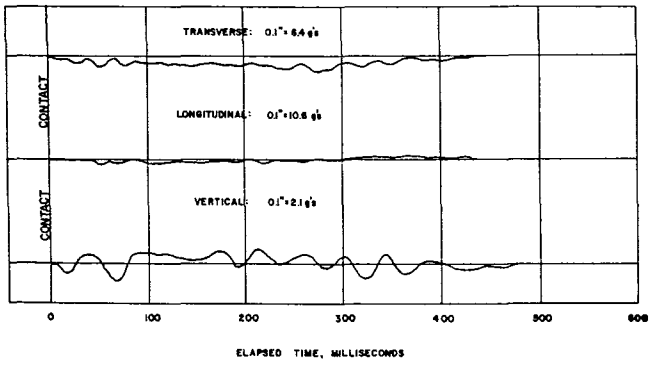

Figure A10. Impact-o-graph acceleration records, Test 1146-4.

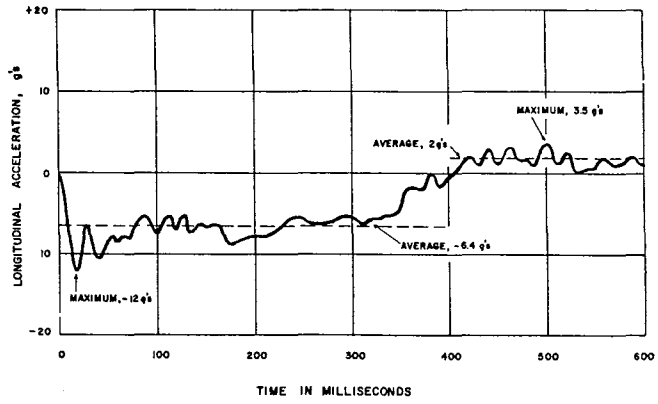

Figure A13. Enlargement of longitudinal impact-o-graph, Test 1146-5.